death was also considered to represent necrotic cell death. These results indicate that CypD (and the CsA-sensitive mPT) is involved in necrotic cell death induced by oxygen radicals or Ca^{2+} overload.

Suppression of A23187-induced cell death by CypD deficiency seemed likely to be due to inhibition of the mPT. To determine whether A23187-induced mPT is suppressed by CypD deficiency in cells, we monitored mitochondrial $\Delta\Psi$ and Ca^{2+} accumulation in the presence of A23187. Hepatocytes were loaded with the $\Delta\Psi$ markers tetramethylrhodamine methylester (TMRM) or Mito Tracker Orange CMTM Ros, and treated with A23187, after which the fluorescence intensity was monitored by real-time imaging. Addition of A23187 caused rapid loss of $\Delta\Psi$ in control (wild-type) hepatocytes, whereas CypD-deficient hepatocytes maintained $\Delta\Psi$ for much longer periods of time (Fig. 3g–i and Supplementary Fig. 5). The addition of CCCP (carbonyl cyanide m-chlorophenyl-hydrazone), a protonophore, completely dissipated $\Delta\Psi$. Mitochondrial accumulation of Ca^{2+} was investigated using Rhod2-AM[16]. After A23187 treatment, CypD-deficient hepatocytes showed a rapid increase in Rhod2 fluorescence intensity, but wild-type hepatocytes showed only a marginal increase (Fig. 3j–l). The validity of using Rhod2 as an indicator of mitochondrial Ca^{2+} under these conditions was confirmed using Ru360, an inhibitor of the mitochondrial calcium uniporter (Fig. 3l). These results indicate that compared to control hepatocytes, CypD-deficient hepatocytes absorb a larger amount of cytosolic Ca^{2+} into their mitochondria without loss of mitochondrial $\Delta\Psi$; this is consistent with the results obtained using isolated mitochondria, and suggests that A23187 induces CypD-dependent mPT in cells.

Finally, we investigated the role of CypD in ischaemia/reperfusion (I/R) injury, in which disturbance of Ca^{2+} homeostasis and generation of reactive oxygen species have been implicated[17]. Many reports have described a protective effect of CsA against I/R injury[18–21]. First, we investigated whether CypD-deficient mitochondria showed resistance to anoxia/reoxygenation-induced injury, which simulates I/R-induced injury *in vivo*. Isolated mitochondria from control and CypD-deficient mice were subjected to anoxia for 30 min, followed by reoxygenation. Control mitochondria, but not CypD-deficient mitochondria, showed loss of $\Delta\Psi$ (Fig. 4a), swelling (Fig. 4b), leakage of mitochondrial asparatate aminotransferase (mAST) (Fig. 4c), and a severe decrease in respiratory control rate (Fig. 4d), indicating that CypD-deficient mitochondria are more resistant to anoxia/reoxygenation injury than control mitochondria.

We next examined the effect of CypD on cardiac I/R injury, because the heart has high levels of CypD (see Supplementary Fig. 1d). Several functional parameters assessed by echocardiography showed no differences between the resting hearts of control and CypD-deficient mice (see Supplementary Table). Mice were then subjected to 30 min of left coronary artery occlusion followed by 2 h of reperfusion. The size of the area at risk, identified by the absence of Evans blue staining, was not significantly different between control and CypD-deficient hearts (Fig. 4f). In control hearts, I/R injury caused significant necrotic damage, as evidenced by a large area of myocardium that was negative for triphenyltetrazolium chloride (TTC) staining (Fig. 4e, g). In CypD-deficient hearts, however, the infarct area was dramatically reduced (Fig. 4e, g). Consistently, lactate dehydrogenase (LDH) release due to disruption of the plasma membrane was almost completely inhibited in CypD-deficient hearts (Fig. 4h). These results indicate that lack of CypD can markedly reduce cardiac I/R injury.

An increase in the permeability of the outer mitochondrial membrane is central to apoptotic signalling, and is directly regulated by the Bcl-2 family of proteins[1]. It has been suggested that the mPT plays a role in apoptotic mitochondrial membrane permeabilization[22]. However, we show here that cytochrome *c* release induced by Bid and Bax is not blocked by CypD deficiency and that CypD deficiency does not affect many forms of apoptotic cell death, indicating that the CypD-dependent mPT does not play a significant role in apoptosis in general; however, this does not exclude the possibility that certain forms of apoptosis are mediated by the mPT, and thereby inhibited by CsA. On the other hand, CypD deficiency blocks Ca^{2+}-induced and oxidative stress-induced cytochrome *c* release from isolated mitochondria and also prevents necrotic cell death induced by these stimuli; this indicates that the CypD-dependent mPT is a critical event in some forms of cellular

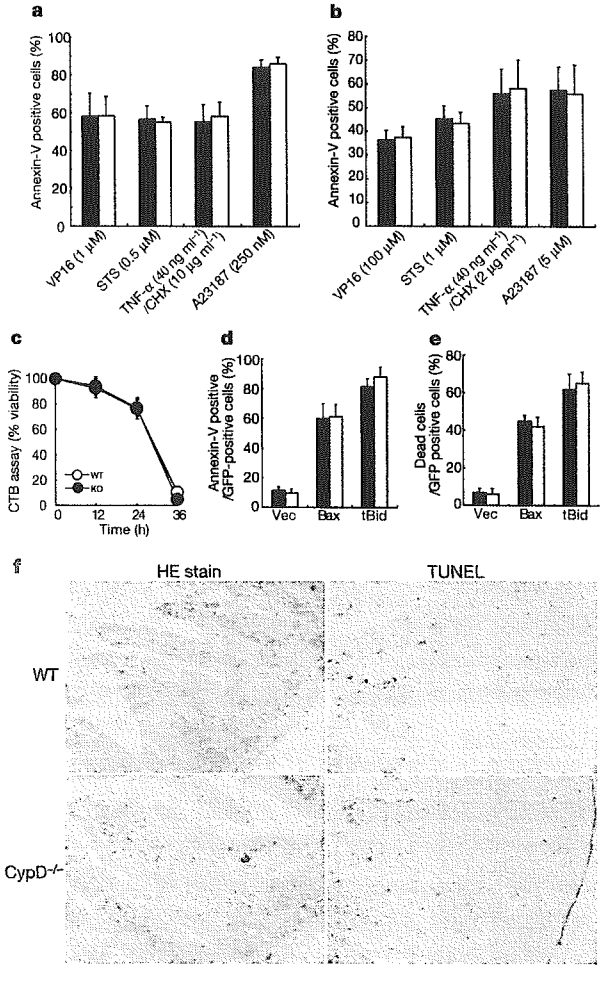

Figure 2 No resistance of Cyp $D^{-/-}$ cells to multiple apoptotic stimuli **a**, **b**, Susceptibility of primary thymocytes and MEFs to various apoptotic stimuli. Wild-type (black) and Cyp $D^{-/-}$ (grey) thymocytes (**a**) and MEFs (**b**) were exposed to apoptosis-inducing reagents for 24 h, and apoptotic cells were assessed by Annexin-V staining. Reagents: etoposide (VP16), staurosporin (STS), tumour-necrosis factor-α (TNF-α) + cycloheximide (CHX), A23187. **c**, Susceptibility of primary hepatocytes to 10 μM STS. Wild-type and $CypD^{-/-}$ hepatocytes were treated with STS for 36 h and cell death was assessed using the CTB assay. Data shown as mean ± s.e.m. **d**, **e**, No effect of CypD deficiency on Bax- or tBid-induced death of MEFs and hepatocytes. Immortalized MEFs (**d**) and primary cultured hepatocytes (**e**) were transiently transfected with DNA for Bax (1 μg) or tBid (1 μg) plus enhanced green fluorescent protein (EGFP, 0.5 μg) for 24 h, and cells were stained with Cy3-conjugated Annexin-V. The percentage of Annexin-V positive cells was calculated relative to all GFP-positive cells. Data shown as mean ± s.e.m. **f**, No effect of CypD deficiency on X-ray-induced apoptosis in the small intestine. Wild-type and $CypD^{-/-}$ mice were exposed to 10 Gy irradiation. After 72 h, a segment of the small intestine was excised and subjected to haematoxylin-eosin (HE) and TUNEL staining.

necrosis. Notably, overexpressed CypD can induce necrosis[23].

We showed that lack of CypD markedly suppresses cardiac I/R injury (which mimics cardiac infarction). In I/R injury, production of reactive oxygen species and Ca^{2+} overload are known to be key events[17]. Our results indicate that CypD-deficient mitochondria can accumulate excess Ca^{2+} without loss of $\Delta\Psi$ and that they also tolerate oxygen radical-induced damage. Consistently, CypD-deficient hepatocytes accumulated more Ca^{2+} than wild-type hepatocytes, and were significantly more resistant to A23187- and H_2O_2-induced death. Thus, the CypD-dependent mPT is a critical event in I/R injury, suggesting that CypD and the mPT may be important therapeutic targets for preventing myocardial infarction. □

Methods

Generation of cyclophilin D-deficient mice

A genomic clone (pKOS 63) containing the CypD locus was isolated from a 129/J mouse genomic library. Lex-1 embryonic stem (ES) cells (derived from the 129SvEvBrd strain)

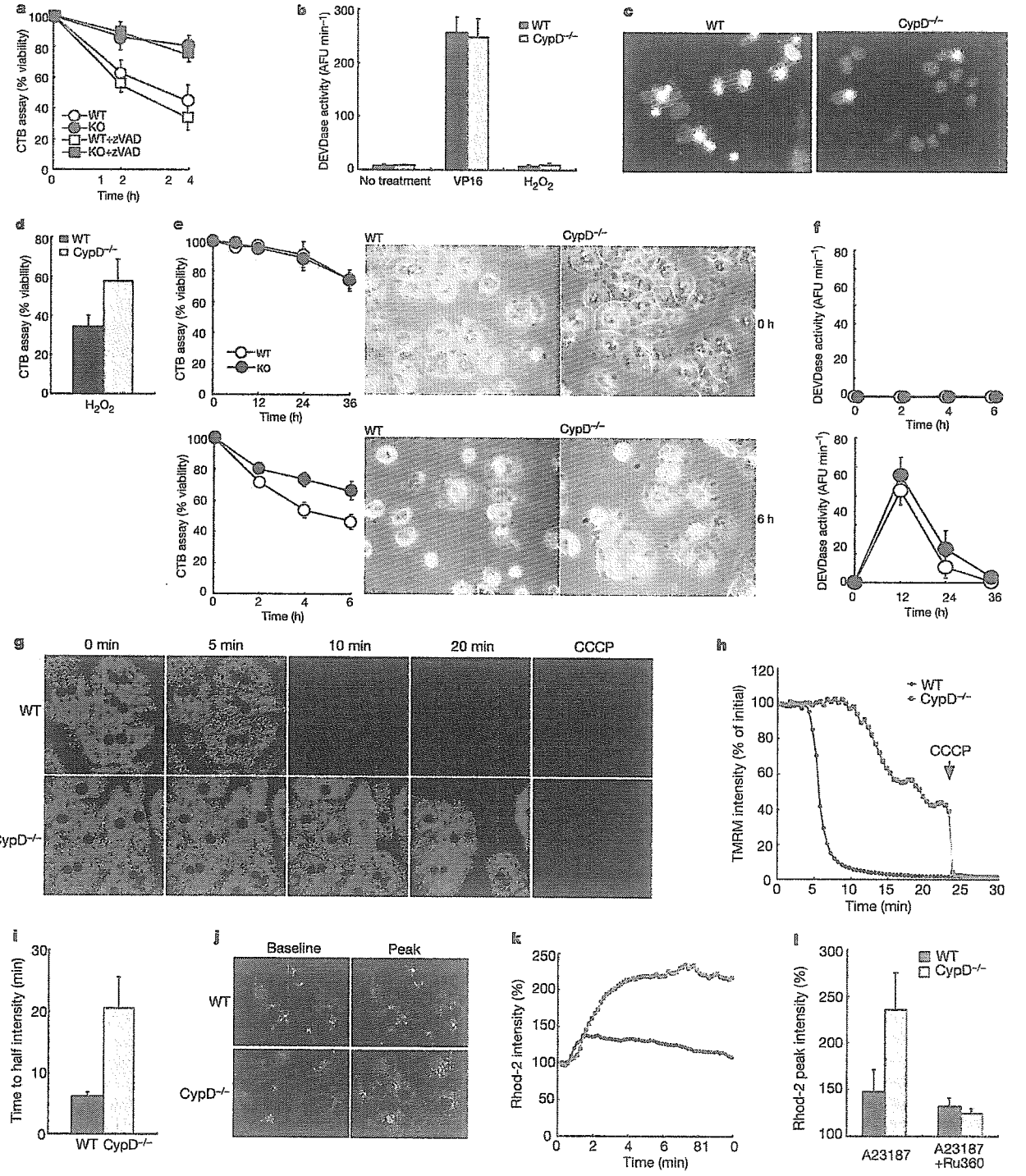

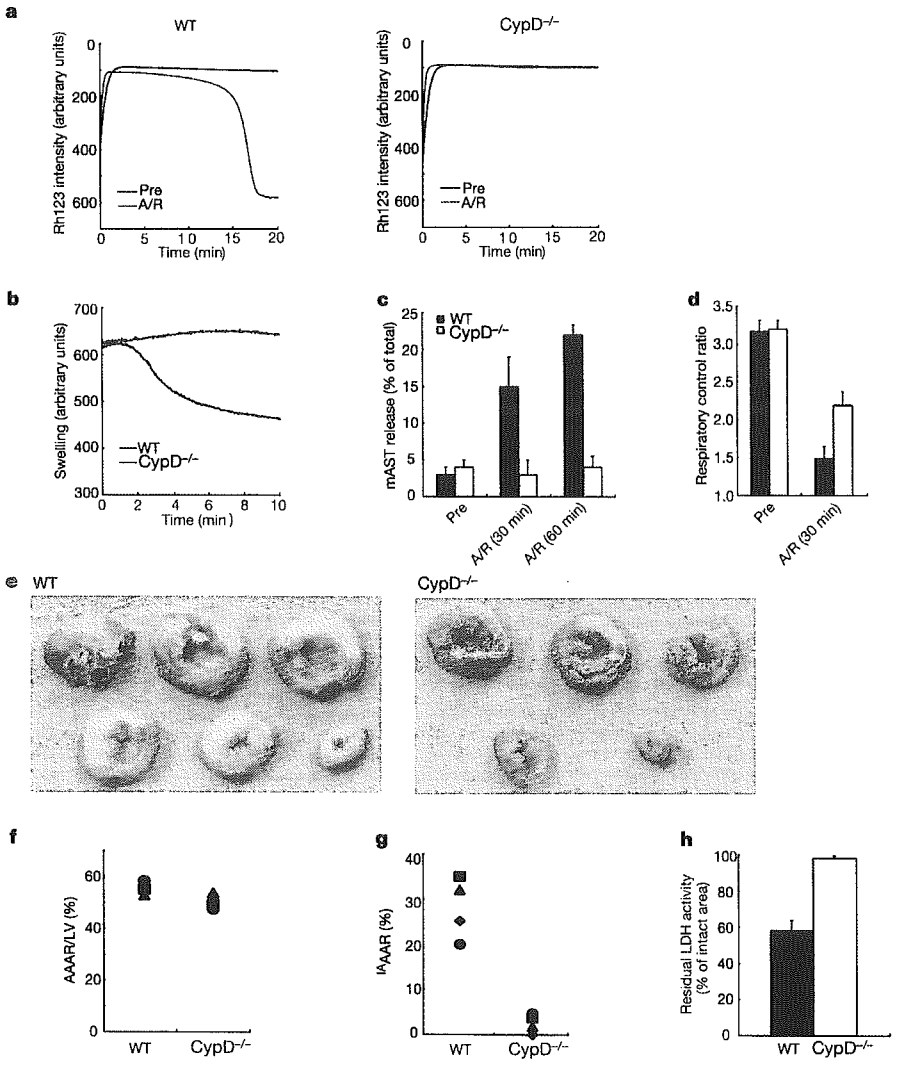

Figure 4 Prevention of cardiac ischaemia/reperfusion injury in CypD$^{-/-}$ mice. **a**–**d**, Absence of mitochondrial damage induced by anoxia/reoxygenation (A/R) in CypD$^{-/-}$ mitochondria. Isolated mitochondria were treated without (Pre) or with anoxia for 30 min followed by reoxygenation for the indicated times. The $\Delta\Psi$ (**a**), swelling (**b**), mAST release (**c**), and respiratory control ratio (state 3/state 4) (**d**) were measured. Data shown as mean ± s.e.m. **e**–**h**, Reduction of cardiac I/R injury in CypD$^{-/-}$ mice. **e**, Representative slices of a heart subjected to I/R. The slices were double-stained with Evans blue (blue) and TTC (red). The infracted region was not stained (white). **f**, The area at risk/left ventricle (AAR/LV) and (**g**) the infarct area/area at risk (IA/AAR). Data are shown for four independent experiments. **h**, The ratio of residual LDH activity in the IA/non-ischaemic area. Data shown as mean ± s.e.m.

Figure 3 Resistance of CypD$^{-/-}$ cells to necrosis induced by reactive oxygen species and Ca^{2+} overload. **a**–**d**, Reduction of H_2O_2-induced necrotic cell death by CypD deficiency. Wild-type (WT) and CypD$^{-/-}$ MEFs (**a**–**c**) and hepatocytes (**d**) were exposed to H_2O_2 (**a**–**c**, 0.75 mM for 24 h; **d**, 0.5 mM for 4 h), and the extent of cell death was assessed by CTB assay (**a**, **d**). zVAD is a pan-caspase inhibitor. **b**, Caspase activation in wild-type (black) and CypD$^{-/-}$ (grey) hepatocytes after treatment with 0.75 mM H_2O_2 was assessed at 16 h. Treatment with VP16 (100 μM) for 16 h was used as a positive control for caspase activation. **c**, Representative nuclear changes visualized by staining with Hoechst 33342 (blue) and PI (red) at 12 h. Data shown as mean ± s.e.m. **e**, WT (filled circles) and CypD$^{-/-}$ (open circles) hepatocytes left untreated (top panel) or treated with 2 μM A23187 (bottom panel), measured using the CTB assay. Data shown as mean ± s.e.m. Phase contrast microscopy images at 0 h and 6 h are shown. **f**, Assessment of caspase activation in response to 2 μM A23187 (left panel); treatment with 40 ng ml^{-1} TNF-α + 10 μg ml^{-1} CHX was used as a positive control for caspase activation (right panel). Data shown as mean ± s.e.m. **g**–**i**, Reduced $\Delta\Psi$ loss in CypD$^{-/-}$ hepatocytes (preloaded with TMRM) treated with 10 μM A23187. TMRM fluorescence intensity was monitored by laser scanning confocal microscopy. Representative real-time images (**g**), average TMRM intensity of individual WT (blue) and CypD$^{-/-}$ (pink) cells (**h**), and the half-life time of the fluorescence intensity of individual cells (**i**) are shown. Data shown as mean ± s.d. The arrow in (**h**) indicates the addition of 5 μM CCCP, which completely dissipated $\Delta\Psi$. **j**–**l**, Increased A23187-induced mitochondrial Ca^{2+} uptake by CypD$^{-/-}$ hepatocytes. Cells were loaded with Rhod2-AM and treated with 10 μM A23187. Rhod2 fluorescence intensity was monitored by laser scanning confocal microscopy. Representative images of baseline and peak fluorescence are shown (**j**). Average (**k**) and peak (**l**) fluorescence intensities of cells are shown (mean ± s.d.). In (**l**), hepatocytes were loaded with Rhod2-AM in the presence of 1 μM Ru360.

were electroporated with the targeting vector and selected by G418. ES clones with the targeted CypD allele were screened by polymerase chain reaction (PCR) and Southern blotting analysis. Heterozygous mutant ES cells were injected into C57BL/6J blastocysts. Germline transmission of mutant alleles to F_1 offspring was confirmed by PCR and Southern blotting, and F_2 offspring from heterozygous intercrosses were genotyped by PCR and Southern blotting.

Genotyping by PCR

The CypD locus was genotyped by PCR. The wild-type allele (553 base pairs, bp) was detected using a forward primer (5′-GCAGATCAAGCTCCCGACTG-3′) and a reverse primer (5′-ACTTGGGAAGCCGAGGTG-3′). To detect the mutant allele (206 bp), a neomycin-specific reverse primer (5′-GCAGCGCATCGCCTTCTATC-3′) was used in combination with the wild-type reverse primer described above.

Antibodies

Anti-mouse CypD antibody was produced using a peptide (amino acids 43–57) of CypD. Anti-cytochrome c, anti-cyclophilin A and anti-GAPDH antibodies were purchased from Pharmingen, UpState and Biogenesis, respectively.

Mitochondrial biochemical parameters

Mitochondria were isolated from mouse livers as described previously[24]. In all experiments, except for assessment of respiration, mitochondria were in medium containing 0.3 mM mannitol, 10 mM potassium HEPES (pH 7.4), 0.2 mM EDTA, 0.1% fatty acid-free BSA, 300 μM potassium phosphate (pH 7.4) and 4.2 mM succinate.

Mitochondrial PPIase activity was measured as described previously[25], except that the final concentration of the synthetic peptide substrate (succinyl-Ala-Ala-Pro-Phe-4-nitroanilide) was 75 μM. The activity was expressed as K/K_0, where K and K_0 are the first-order rate constants in the presence and absence of the mitochondrial lysate, respectively. The mitochondrial membrane potential ($\Delta\Psi$) was assessed by measuring the $\Delta\Psi$-dependent uptake of rhodamine 123 (Rh123, ref. 24). Mitochondrial swelling was monitored by the decrease of 90° light scatter at 520 nm, which was determined using a spectrophotometer (Hitachi F-4500). Mitochondrial respiration was measured with an O_2 electrode (Rank Brothers) in respiration buffer[24]. The external mitochondrial Ca^{2+} concentration was monitored using a Ca^{2+}-specific electrode (Orion). The amount of intra-mitochondrial Ca^{2-} was measured using $^{45}Ca^{2+}$. Isolated mitochondria were incubated with $^{45}Ca^{2+}$ for 25 min, and then the mitochondria (1 mg protein) were centrifuged at 12,000*g* for 3 min. The pellet and supernatant fractions were collected and their radioactivity measured using a liquid scintillation counter (Wallac 1409). Cytochrome *c* release was determined as previously described[13].

In anoxia/reoxygenation experiments, mitochondria were suspended in a tube and treated with 100% N_2 gas. The gas-saturated tube was sealed with parafilm and left for 30 min, and the mitochondria were then reoxygenated by shaking in a 12-well plate at room temperature for 30 min.

Cell death assay

Primary cultures of MEFs were obtained from CypD-deficient and control littermate embryos at embryonic day 14.5. MEFs immortalized by SV40 T antigen were also used. Hepatocytes were isolated from CypD-deficient mice and their control littermates at 3–4 months of age using the retrograde two-step collagenase perfusion technique[26]. Cell viability was assessed by propodium iodide (PI) staining, Annexin-V staining or the cell titer blue (CTB) assay. Briefly, cells were stained with 1 μM PI or 1 μM Cy3-conjugated Annexin-V for 5 min at room temperature and were analysed using a flow cytometer (Becton-Dickinson). The CTB assay, which measures the metabolic activity of viable cells, was carried out using Cell Titer Blue reagent (Promega). The nuclear morphology was observed with 10 μM Hoechst 33342 and 1 μM PI staining as described previously[27]. DEVDase activity (cleavage of the caspase-3 substrate DEVD-amc) was measured as described elsewhere[28].

Q4

Laser scanning confocal microscopy

Hepatocytes were cultured in covered glass-bottomed 24-well dishes coated with type I collagen (Iwaki glass) for 16–20 h. To monitor mitochondrial $\Delta\Psi$, hepatocytes were loaded with 0.25 μM TMRM (Molecular Probes) as described previously[29]. To monitor the mitochondrial Ca^{2+} level, hepatocytes were loaded with 5 μM Rhod2-AM (Molecular Probes) in culture medium containing 0.05% Pluronic F-127 (Molecular Probes) and 0.1 mM sulfypizrazone for 2 h at 4 °C for mitochondria-selective loading as described previously[16].

Ischaemia/reperfusion experiments

Using CypD-deficient and wild-type littermate mice at 10–12 weeks of age, ischaemia/reperfusion of the heart was performed as described previously[30]. Briefly, under general anaesthesia with mechanical ventilation, a silk thread (7-0) was passed around the left coronary artery (LCA) about 1 mm distal to the LCA origin to make a snare. After 30 min ligation of the LCA, the snare was released for 2 h. The infarct size was evaluated by double staining using Evans blue dye and triphenyltetrazolium chloride (TTC). The area at risk was defined as the ratio of the area of the ischaemic region to the left ventricular area, and the infarct size was defined as the ratio of the area of the infracted region to that of the ischaemic region.

Statistical evaluation

Statistical evaluation was performed by unpaired *t*-tests. Data are presented as mean ± s.e.m. except for the data shown in Fig. 3i and l, which are shown as mean ± s.d.

Received 2 September 2004; accepted 4 January 2005; doi:10.1038/nature03317.

1. Tsujimoto, Y. Cell death regulation by the Bcl-2 protein family in the mitochondria. *J. Cell. Physiol.* **195,** 158–167 (2003).
2. Green, D. R. & Kroemer, G. The pathophysiology of mitochondrial cell death. *Science* **305,** 626–629 (2004).
3. Halestrap, A. P., McStay, G. P. & Clarke, S. J. The permeability transition pore complex: another view. *Biochimie* **84,** 153–166 (2002).
4. Crompton, M. On the involvement of mitochondrial intermembrane junctional complexes in apoptosis. *Curr. Med. Chem.* **10,** 1473–1484 (2003).
5. Kokoszka, J. E. *et al.* The ADP/ATP translocator is not essential for the mitochondrial permeability transition pore. *Nature* **427,** 461–465 (2004).
6. Halestrap, A. P. Mitochondrial permeability: dual role for the ADP/ATP translocator? *Nature* [online] **430,** 983 (2004) (doi:10.1038/nature02816).
7. Galat, A. & Metcalfe, S. M. Peptidylproline cis/trans isomerases. *Prog. Biophys. Mol. Biol.* **63,** 67–118 (1995).
8. Broekemeier, K. M., Dempsey, M. E. & Pfeiffer, D. R. Cyclosporin A is a potent inhibitor of the inner membrane permeability transition in liver mitochondria. *J. Biol. Chem.* **264,** 7826–7830 (1989).
9. He, L. & Lemasters, J. J. Regulated and unregulated mitochondrial permeability transition pores: a new paradigm of pore structure and function? *FEBS Lett.* **512,** 1–7 (2002).
10. Scorrano, L. *et al.* A distinct pathway remodels mitochondrial cristae and mobilizes cytochrome c during apoptosis. *Dev. Cell* **2,** 55–67 (2002).
11. Wei, M. C. *et al.* Proapoptotic BAX and BAK: a requisite gateway to mitochondrial dysfunction and death. *Science* **292,** 727–730 (2001).
12. Narita, M. *et al.* Bax interacts with the permeability transition pore to induce permeability transition and cytochrome c release in isolated mitochondria. *Proc. Natl Acad. Sci. USA* **95,** 14681–14686 (1998).
13. Eskes, R. *et al.* Bax-induced cytochrome C release from mitochondria is independent of the permeability transition pore but highly dependent on Mg^{2+} ions. *J. Cell Biol.* **143,** 217–224 (1998).
14. Finucane, D. M., Bossy-Wetzel, E., Waterhouse, N. J., Cotter, T. G. & Green, D. R. Bax-induced caspase activation and apoptosis via cytochrome c release from mitochondria is inhibitable by Bcl-xL. *J. Biol. Chem.* **274,** 2225–2233 (1999).
15. von Ahsen, O. *et al.* Preservation of mitochondrial structure and function after Bid- or Bax-mediated cytochrome c release. *J. Cell Biol.* **150,** 1027–1036 (2000).
16. Trollinger, D. R., Cascio, W. E. & Lemasters, J. J. Selective loading of Rhod 2 into mitochondria shows mitochondrial Ca^{2+} transients during the contractile cycle in adult rabbit cardiac myocytes. *Biochem. Biophys. Res. Commun.* **236,** 738–742 (1997).
17. Weiss, J. N., Korge, P., Honda, H. M. & Ping, P. Role of the mitochondrial permeability transition in myocardial disease. *Circ. Res.* **93,** 292–301 (2003).
18. Shimizu, S. *et al.* Beneficial effects of cyclosporine on reoxygenation injury in hypoxic rat liver. *Transplantation* **57,** 1562–1566 (1994).
19. Javadov, S. A. *et al.* Ischaemic preconditioning inhibits opening of mitochondrial permeability transition pores in the reperfused rat heart. *J. Physiol. (Lond.)* **549,** 513–524 (2003).
20. Matsumoto, S., Friberg, H., Ferrand-Drake, M. & Wieloch, T. Blockade of the mitochondrial permeability transition pore diminishes infarct size in the rat after transient middle cerebral artery occlusion. *J. Cereb. Blood Flow Metab.* **19,** 736–741 (1999).
21. Khaspekov, L., Friberg, H., Halestrap, A., Viktorov, I. & Wieloch, T. Cyclosporin A and its nonimmunosuppressive analogue N-Me-Val-4-cyclosporin A mitigate glucose/oxygen deprivation-induced damage to rat cultured hippocampal neurons. *Eur. J. Neurosci.* **11,** 3194–3198 (1999).
22. Zamzami, N. & Kroemer, G. The mitochondrion in apoptosis: how Pandora's box opens. *Nature Rev. Mol. Cell Biol.* **2,** 67–71 (2001).
23. Li, Y., Johnson, N., Capano, M., Edwards, M. & Crompton, M. Cyclophilin-D promotes the mitochondrial permeability transition but has opposite effects on apoptosis and necrosis. *Biochem. J.* **383,** 101–109 (2004).
24. Shimizu, S. *et al.* Bcl-2 prevents apoptotic mitochondrial dysfunction by regulating proton flux. *Proc. Natl Acad. Sci. USA* **95,** 1455–1459 (1998).
25. Fischer, G., Wittmann-Liebold, B., Lang, K., Kiefhaber, T. & Schmid, F. X. Cyclophilin and peptidyl-prolyl *cis-trans* isomerase are probably identical proteins. *Nature* **337,** 476–478 (1989).
26. Hatano, E. *et al.* The mitochondrial permeability transition augments Fas-induced apoptosis in mouse hepatocytes. *J. Biol. Chem.* **275,** 11814–11823 (2000).
27. Shinzawa, K. & Tsujimoto, Y. PLA2 activity is required for nuclear shrinkage in caspase-independent cell death. *J. Cell Biol.* **163,** 1219–1230 (2003).
28. Shimizu, S., Eguchi, Y., Kamiike, W., Matsuda, H. & Tsujimoto, Y. Bcl-2 expression prevents activation of the ICE protease cascade. *Oncogene* **12,** 2251–2257 (1996).
29. Byrne, A. M., Lemasters, J. J. & Nieminen, A. L. Contribution of increased mitochondrial free Ca^{2+} to the mitochondrial permeability transition induced by tert-butylhydroperoxide in rat hepatocytes. *Hepatology* **29,** 1523–1531 (1999).
30. Yamashita, N. *et al.* Exercise provides direct biphasic cardioprotection via manganese superoxide dismutase activation. *J. Exp. Med.* **189,** 1699–1706 (1999).

Supplementary Information accompanies the paper on **www.nature.com/nature.**

Acknowledgements We are grateful to K. Tagawa for helpful discussion and C. Thompson for providing Bak-deficient mice. CypD-deficient mice were developed in collaboration with Lexicon Genetics Incorporated. This study was supported in part by a grant for Scientific Research on Priority Areas, a grant for Center of Excellence Research, a grant for the 21st century COE Program, a grant for Scientific Research from the Ministry of Education, Science, Sports, and Culture of Japan, and by a grant for Research on Dementia and Fracture from the Ministry of Health, Labour and Welfare of Japan.

Competing interests statement The authors declare that they have no competing financial interests.

Correspondence and requests for materials should be addressed to Y.T. (tsujimot@gene.med.osaka-u.ac.jp)

Journal of Neurochemistry, 2004, **90**, 1402–1413 doi:10.1111/j.1471-4159.2004.02597.x

PEN-2 enhances γ-cleavage after presenilin heterodimer formation

Hirohisa Shiraishi,*,† Xiaorei Sai,*,[1] Hua-Qin Wang,‡ Yasuhiro Maeda,§ Yukihisa Kurono,§ Masaki Nishimura,‡ Katsuhiko Yanagisawa* and Hiroto Komano*

**Department of Dementia Research, National Institute for Longevity Sciences, Morioka, Obu, Aichi, Japan*

†Organization for Pharmaceutical Safety and Research of Japan, Chiyoda-ku, Tokyo, Japan

‡Molecular Neuroscience Research Center, Shiga University of Medical Science, Otsu, Shiga, Japan

§Faculty of Pharmaceutical Sciences, Nagoya City University, Nagoya, Aichi, Japan

Abstract

The presenilin (PS) complex, including PS, nicastrin, APH-1 and PEN-2, is essential for γ-secretase activity, which is required for amyloid β-protein (Aβ) generation. However, the precise individual roles of the three cofactors in the PS complex in Aβ generation remain to be clarified. Here, to distinguish the roles of PS cofactors in γ-secretase activity from those in PS endoproteolysis, we investigated their roles in the γ-secretase activity reconstituted by the coexpression of PS N- and C-terminal fragments (NTF and CTF) in PS-null cells. We demonstrate that the coexpression of PS1 NTF and CTF forms the heterodimer and restores Aβ generation in PS-null cells. The generation of Aβ was saturable at a certain expression level of PS1 NTF/CTF, while the overexpression of PEN-2 alone resulted in a further increase in Aβ generation. Although PEN-2 did not enhance PS1 NTF/CTF heterodimer formation, PEN-2 expression reduced the IC_{50} of a specific γ-secretase inhibitor, a transition state analogue, for Aβ generation, suggesting that PEN-2 expression enhances the affinity or the accessibility of the substrate to the catalytic site. Thus, our results strongly suggest that PEN-2 is not only an essential component of the γ-secretase complex but also an enhancer of γ-cleavage after PS heterodimer formation.

Keywords: Alzheimer's disease, amyloid β-protein, nicastrin, PEN-2, APH-1, presenilin.

J. Neurochem. (2004) **90,** 1402–1413.

In the brains of patients with Alzheimer's disease, the fundamental neuropathological change is the abnormal deposition of amyloid β-protein (Aβ) (for review, see Selkoe 1999). Aβ is generated from β-amyloid precursor protein (APP) through its sequential proteolytic cleavage catalysed by β- and γ-secretases (for review, see Selkoe 1999). β-secretase was identified as a membrane-tethered aspartyl protease (Vassar *et al.* 1999), whereas the molecules responsible for γ-secretase activity were found to be the presenilin (PS) complex, including PS, nicastrin (NCT) (Yu *et al.* 2000b), APH-1 (Goutte *et al.* 2002) and PEN-2 (Francis *et al.* 2002).

Mutations in the PS genes, *PS1* and *PS2*, cause early onset familial Alzheimer's disease (reviewed in Selkoe 1999). PS is required not only for γ-secretase activity (De Strooper *et al.* 1998; Herreman *et al.* 2000; Zhang *et al.* 2000) but also several intramembranous cleavages, including those of APP named as ε-cleavage (Gu *et al.* 2001; Sastre *et al.* 2001; Weidemann *et al.* 2002), Notch (De Strooper *et al.* 1999; Zhang *et al.* 2000), ErbB-4 (Lee *et al.* 2001; Ni *et al.* 2001), Cadherin (Marambaud *et al.* 2002, 2003), and CD44 (Lammich *et al.* 2002; Murakami *et al.* 2003). These results suggest that PS-mediated intramembranous cleavage plays a critical role in biological functions. PS has been proposed to have the catalytic site of γ-secretase; it contains two conserved, essential aspartate residues in adjacent transmembrane domains that may define a novel aspartyl protease active site (Wolfe *et al.* 1999; Li *et al.* 2000b; Steiner *et al.* 2000; Weihofen *et al.* 2002). PS is processed to an active,

Received February 18, 2004; revised manuscript received April 27, 2004; accepted May 11, 2004.

Address correspondence and reprint requests to Hiroto Komano, Department of Dementia Research, National Institute for Longevity Sciences, 36-3 Gengo, Morioka, Obu, Aichi 474-8522, Japan.
E-mail: hkomano@nils.go.jp

[1]The present address of Xiaorei Sai is Laboratory for Sensory Development, RIKEN-Center for Developmental Biology, Chuo-ku, Kobe 656-0047, Japan.

Abbreviations used: Aβ, amyloid β-protein; APP, β-amyloid precursor protein; CTF, C-terminal fragment; DAPT, *N*-[*N*-(3,5-difluorophenylacetyl)-L-alanyl]-*S*-phenylglycine *t*-butyl ester; ELISA, enzyme-linked immunosorbent assay; IC50, 50% inhibitory concentration; NCT, nicastrin; NTF, N-terminal fragment; PS, presenilin; RIPA, radioimmunoprecipitation assay.

stable form by endoproteolysis and the cellular level of processed PS is tightly limited (Ratovitski *et al.* 1997; Thinakaran *et al.* 1997). The processed PS resides in a high molecular weight complex that includes mature glycocylated NCT, APH-1 and PEN-2 (Yu *et al.* 2000b; Edbauer *et al.* 2002; Esler *et al.* 2002; Yang *et al.* 2002; Kimberly *et al.* 2003; Takasugi *et al.* 2003).

Several lines of evidence have clearly established that NCT, APH-1 and PEN-2 (collectively named PS cofactors in this study) are required for PS processing and the formation of the active γ-secretase complex (Francis *et al.* 2002; Lee *et al.* 2002; Steiner *et al.* 2002; Edbauer *et al.* 2003; Hu and Fortini 2003; Kim *et al.* 2003; Kimberly *et al.* 2003; Luo *et al.* 2003; Takasugi *et al.* 2003). In addition, reconstitution experiments in yeast demonstrated that the coexpression of all four components is necessary and sufficient for the reconstitution of γ-secretase activity (Edbauer *et al.* 2003). However, the precise roles of PS cofactors in Aβ generation remain to be elucidated because it is not yet conclusive whether the cofactors are only necessary for PS endoproteolysis and the formation of the active γ-secretase or whether they also play a role in Aβ generation after the formation of the γ-secretase complex. Here, we demonstrate that the coexpression of PS1 N- and C-terminal fragments (NTF and CTF) in PS-null cells (PS1/PS2 double-deficient cells) restores Aβ generation similarly to the expression of PS holoprotein. As the coexpression of PS1 NTF and CTF in PS-null cells allows us to distinguish the roles of PS cofactors in γ-secretase activity from those in PS endoproteolysis, we investigated their roles in the γ-secretase activity reconstituted by the coexpression of PS NTF and CTF in PS-null cells. We noted that PEN-2 expression results in an increase in the extent of Aβ generation restored by the coexpression of PS NTF and CTF in PS-null cells. Thus, we concluded that PEN-2 enhances PS-mediated γ-cleavage after PS NTF/CTF heterodimer formation.

Experimental procedures

Antibodies, reagents and cell lines

The monoclonal antibody 6E10 specific to human Aβ1–17 was purchased from Signet Laboratories, Inc. (Redham, MA, USA). The other Aβ antibodies have all been characterized previously (Asami-Odaka *et al.* 1995). The affinity-purified rabbit antibody, B12/4, was raised against 20 C-terminal amino acid residues of APP695 (De Strooper *et al.* 1995). The anti-APP N-terminal antibody was purchased from Sigma (St Louis, MO, USA). The rat anti-PS1 antibody (for NTF of PS1) and the mouse anti-PS1 loop monoclonal antibody were purchased from Chemicon (Temecula, CA, USA). An anti-NCT antibody was purchased from Affinity BioReagents Inc. (Golde, CO, USA) and Sigma. An anti-myc antibody was purchased from MBL (Nagoya, Japan). Affinity-purified rabbit antibody 369 was raised against the C-terminal residues of APP695 (Buxbaum *et al.* 1990). The rabbit anti-PEN-2 antibody was purchased from Zymed Laboratories Inc. (South San Francisco, CA, USA). PS1/PS2 double-deficient murine fibroblasts (PS-null cells) and wild-type murine fibroblasts immortalized with a large T antigen were maintained as previously described (Herreman *et al.* 2000; Sai *et al.* 2002). A γ-secretase inhibitor, L-685,458, was purchased from Calbiochem (San Diego, CA, USA), *N*-[*N*-(3,5-difluorophenylacetyl)-L-alanyl]-*S*-phenylglycine *t*-butyl ester (DAPT) was purchased from Peptide Institute Inc. (Osaka, Japan) and Compound-E and WPE-III-31C were purchased from Calbiochem (San Diego, CA, USA).

Plasmids and retrovirus-mediated gene expression

N-terminal FLAG-tagged PEN-2 and C-terminal myc-tagged APH-1b (Francis *et al.* 2002) were amplified from the Hela cell cDNA library (Clontech, Palo Alto, CA, USA) by the PCR method. The primer sequences used for the PCR were as follows: primers for N-terminal FLAG-tagged PEN-2, 5′-TTCTGAATTCAACCTGGAGCGAGTGTCCAATGAG-3′ and 5′-TTTTCTCGAGCCCCAGTATGTGCAGAAGTTGTCA-3′; primers for C-terminal myc-tagged APH-1b, 5′-TTTTAAGCTTGTTTCCGCGGTGGCCATGACT-3′ and 5′-TTTTGAGCTCTCTGGAGCGCTGGTTGTAAAG-3′. PEN-2 was amplified by the PCR method using the primers 5′-CGCGGATCCACCATGAACCTGGAGCGAGTGTCCAAT-3′ and 5′-CGCGGATCCATGAACCTGGAGCGAGTGTCCAATGAGGAGAAATTGA-3′. pMX-F-PEN-2 is a *Bam*HI-*Sal*I fragment carrying the sequence encoding the N-terminal FLAG-tagged PEN-2 and Kozac consensus sequence (CCACC) at the 5′ end inserted into the *Bam*HI and *Sal*I sites of a retrovirus vector, pMX (Onishi *et al.* 1996). pMX-PEN-2 is inserted into the *Bam*HI and *Xho*I sites of a pMX. pMX-APH-1b-myc is a 1.4-kb *Bam*HI-*Sal*I fragment carrying the C-terminal myc-tagged APH-1b inserted into the *Bam*HI and *Sal*I sites of pMX. pMX-NCT is a *Bam*HI-*Not*I fragment carrying NCT inserted into the *Bam*HI and *Sal*I sites of pMX. pMX-PS1 is a *Not*I fragment carrying PS1 inserted into the *Not*I site of pMX. pMX-APP695 was generated as previously described (Komano *et al.* 2002). pMX-PS1D385 A is an *Eco*RI-*Xho*I fragment carrying mutant PS1 D385A (Yu *et al.* 2000a) inserted into the *Eco*RI and *Sal*I sites of pMX. The PS1 NTF was amplified using the primers PS1-NR, 5′-CATGCTCGAGCTATGTTGAGGAGTAAATG-3′ and PS1-NF, 5′-TGCAGAATTCATGACAGAGTTACCTGCA-3′. The PS1 CTF was amplified using the primers PS1-CR, 5′-CATGCTCGAGCTAGATATAAAATTGATGG-3′ and PS1-CF, 5′-TGCAGAATTCATGGTGTGGTTGGTGAATA-3′. The PCR products were digested with *Eco*RI and *Xho*I inserted into pMX. The PS NTF containing D257A and PS1 CTF containing D385A were PCR amplified using the primers described above from pMX-D257A and pMX-PS1D385A, respectively. All resulting constructs were verified by DNA sequencing. Retrovirus-mediated gene expression in cells was carried out as previously reported (Onishi *et al.* 1996; Komano *et al.* 2002). The infection efficiency was nearly 100% in this study, as estimated in a control experiment using pMX-GFP (retroviral vector carrying GFP).

Amyloid β-protein detection and other immunoblotting techniques

The secreted Aβ was determined by ELISA as previously described (Asami-Odaka *et al.* 1995). The capture antibody used was BNT77. The detector antibodies used were horseradish peroxidase-conjugated BA27 (for Aβ40) and horseradish peroxidase-conjugated

BC05 (for Aβ42). ELISA data were statistically analysed by ANOVA using StatView-J.4.11 (Abacus Concepts, Inc., Berkeley, CA, USA). Cultured cells were lysed in ristocetin-induced platelet agglutination (RIPA) buffer (150 mM NaCl, 10 mM Tris/HCl, pH 7.5, 1% Nonidet P-40, 0.1% sodium dodecyl sulphate and 0.2% sodium deoxycholate, a protease inhibitor cocktail) or 1% CHAPSO buffer (1% CHAPSO, 150 mM NaCl, 10 mM Tris/HCl, pH 7.5, 2 mM EDTA, a protease inhibitor cocktail). The RIPA-solubilized proteins were subjected to immunoblotting as previously described (Sudoh *et al.* 1998). The CHAPSO-solubilized proteins were subjected to immunoprecipitation as previously described (Sudoh *et al.* 1998; Li *et al.* 2000a).

Results

PEN-2 expression increases amyloid β-protein generation

We first established the effect of exogenous PEN-2 and/or APH-1b expression (Francis *et al.* 2002) on Aβ generation and PS1 endoproteolysis using fibroblasts retrovirally expressing human PS1, NCT and APP. As previously reported, the coexpression of PEN-2, APH-1b and NCT resulted in significant accumulations of PS1 NTF and CTF, accompanied by the stimulation of NCT maturation (Fig. 1a, lane 4), while no effect of PEN-2 or APH-1b expression alone on the steady-state levels of PS1 NTF and CTF was observed (Fig. 1a) (Kim *et al.* 2003; Kimberly *et al.* 2003; Luo *et al.* 2003; Takasugi *et al.* 2003). It appears that the interaction of NCT, APH-1 and PEN-2 with PS permits autoproteolysis and the stimulation of the intracellular trafficking of the complex leading to NCT maturation. However, unexpectedly, the expression of PEN-2 alone significantly increased both the Aβ40 and Aβ42 levels (two- to threefold) (Figs 1a and b). The degree of this increase was equivalent to (or even higher than) that induced by the coexpression of the three components NCT, APH-1 and PEN-2 (Figs 1a and b). Thus, we decided to characterize the increase in Aβ generation caused by exogenous PEN-2 using fibroblasts expressing APP695 (PS, NCT and APH-1, endogenous levels). As shown in Fig. 1(c), even when NCT, APH-1 and PS were at endogenous levels, exogenous PEN-2 expression increased Aβ generation. PEN-2 expression does not increase the level of α- or β-secretase-cleaved soluble APP (Selkoe 1999), indicating that PEN-2 did not enhance α- and β-secretase cleavage. However, the intracellular levels of the β-secretase-cleaved APP CTF (C99) and the α-secretase-cleaved APP CTF (C83), which are the substrates of γ-secretase (Wolfe *et al.* 1999), were decreased by PEN-2 expression (Fig. 1c). We also confirmed that an increase in Aβ generation by PEN-2 expression is completely dependent on PS, as no Aβ was detected in PS-null cells overexpressing PEN-2 (data not shown). We also obtained results showing that HEK293 or N2a cells retrovirally expressing PEN-2 increased Aβ generation [an increase in Aβ generation by the retroviral expression of PEN-2 relative to mock expression (fold): N2a, 1.8 (Aβ40) and 1.7 (Aβ42), $n = 4$, $p < 0.02$; HEK293 expressing APP 695, 1.6 (Aβ40) and 1.6 (Aβ42), $n = 4$, $p < 0.02$]. This result strongly suggested that an increase in Aβ generation by PEN-2 expression occurs in other cell types.

We next determined the effects of various expression levels of PEN-2, APH-1b or NCT on Aβ generation (Fig. 2a) because the capability of the cofactors to increase Aβ generation may be dependent on their expression levels. For this purpose, using various concentrations of the virus solution containing the cofactor cDNA, we investigated the change in the extent of Aβ generation with the expression level of PEN-2, APH-1 or NCT by the retrovirus-mediated expression method. We found that PEN-2 expression increased Aβ generation in a dose-dependent manner while APH-1b inhibited Aβ generation and NCT expression did not affect Aβ generation. We also excluded the possibility that the presence of the FLAG tag on PEN-2 has an effect of enhancing Aβ generation, because PEN-2 without the FLAG tag also increased Aβ generation, as shown in Fig. 2(b). Therefore, we concluded that the expression of PEN-2 can enhance PS-mediated γ-secretase cleavage but this effect appears not to be associated with the stimulation of PS endoproteolysis as suggested in Fig. 1(a).

Thus, we decided to separate the roles of the PS cofactors in γ-secretase activity from those in PS endoproteolysis.

Coexpression of presenilin 1 N- and C-terminal fragments restores amyloid β-protein generation in presenilin-null cells

Previously, it was shown that the coexpression of PS1 NTF and CTF rescues the *sel-12* egg-laying defect, suggesting that the coexpression of PS1 and CTF forms biologically active PS in cells (Levitan *et al.* 2001). However, it was not clarified whether the coexpression of PS1 NTF and CTF forms active γ-secretase in PS-null cells. Therefore, to distinguish the roles of PS cofactors in the PS endoproteolysis and γ-secretase activity, we first determined whether the coexpression of PS1 NTF and CTF in PS-null cells can restore Aβ generation. As shown in Fig. 3(a), the coexpression of PS1 NTF and CTF induced Aβ generation similarly to the expression of PS1 holoprotein, while the expression of PS1 NTF or CTF alone did not restore Aβ generation. This result clearly indicates that the coexpression of PS1 NTF and CTF leads to the formation of a functional complex for γ-secretase activity. The coexpression of PS1 NTF mutated at Asp257 and CTF or PS NTF and CTF mutated at Asp385 did not induce Aβ generation in PS-null cells (Fig. 3b), clearly indicating that either of the aspartate residues located in putative transmembrane domains 6 (TM6) and 7 (TM7) is necessary for γ-secretase activity mediated by the coexpression of PS1 NTF and CTF. We also investigated whether the γ-secretase activity is dependent on the expression levels of

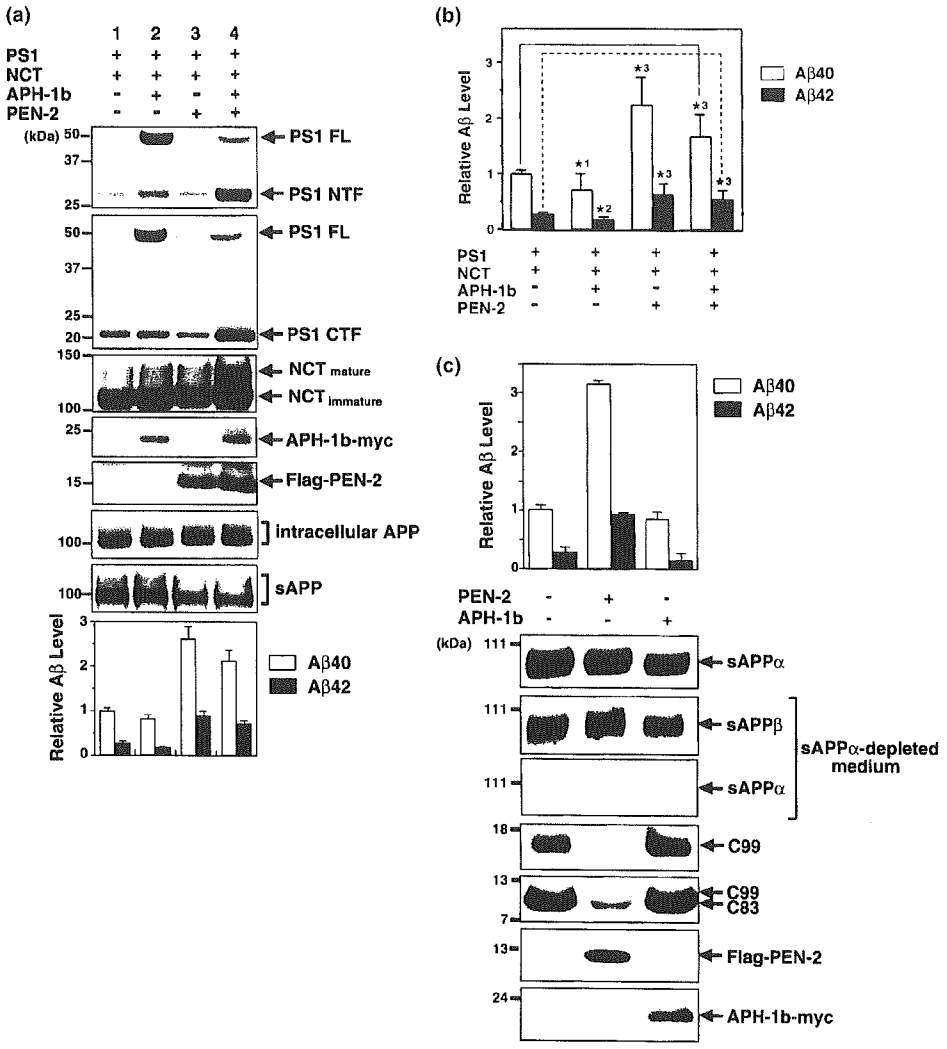

Fig. 1 Exogenous PEN-2 enhances amyloid β-protein (Aβ) generation. (a) Effect of exogenous PEN-2 and/or APH-1b on presenilin (PS)1 endoproteolysis and Aβ generation. Murine fibroblasts (2×10^5) retrovirally expressing β-amyloid precursor protein (APP)695 were plated on a 100-mm tissue culture dish. After the indicated exogenous genes were retrovirally expressed, the RIPA-solubilized lysates (25 μg) were immunoblotted with the anti-PS1 N-terminal fragment (NTF) antibody, anti-PS1 loop antibody, anti-nicastrin (NCT) antibody, anti-FLAG antibody (for FLAG-tagged PEN-2), anti-myc antibody (for myc-tagged APH-1b) and anti-APP antibody, 6E10. Soluble APP (sAPP) was immunoblotted with anti-APP antibody 22C11. Aβ40 and Aβ42 secreted from the cells during a 48-h culture were quantified by ELISA. Values are means ± SD of two independent dishes ($n = 2$). The intensities of the band corresponding to sAPP were quantified densitometrically using NIH Image software (National Institute of Health, Bethesda, MA, USA). The Aβ level was normalized to sAPP in each experiment. The normalized levels were expressed as relative to basal Aβ40 levels obtained from the cells expressing NCT and PS1. +, retrovirus-mediated expression of the indicated exogenous cDNAs; –, mock infection (retroviral vector, pMX, alone). PEN-2, N-terminally FLAG-tagged PEN-2 (FLAG-PEN-2); APH-1b, C-terminally myc-tagged APH-1b (APH-1b-myc); PS1 FL, PS1 full-length; PS1 NTF, PS1 N-terminal fragment; PS1 CTF, PS1 C-terminal fragment. The CTF level of endogenous PS1 in mock-transfected cells (pMX alone) was similar to that of exogenous PS1 observed in lane 1, probably caused by the replacement of the endogenous PS1 with exogenous PS1 as previously shown (Thinakaran *et al.* 1996, 1997) (data not shown). (b) The statistical analysis of Aβ levels of the six independent experiments ($n = 6$). Significant difference at $^{*1}p < 0.05$, $^{*2}p < 0.01$ and $^{*3}p < 0.005$ (Mann–Whitney *U*-test). (c) Exogenous PEN-2 expression alone enhances γ-cleavage. After PEN-2 or APH-1b was retrovirally expressed in fibroblasts (2×10^5) expressing APP695 (PS and NCT, endogenous levels), Aβ40 and Aβ42 secreted from cells during a 48-h culture were quantified by ELISA. The Aβ level was normalized to sAPP in each experiment. The normalized levels were expressed as relative to basal Aβ40 levels obtained from the mock-transfected cells as described in (a). The medium used for the 48-h culture was immunoblotted with 6E10 (for sAPPα). The sAPPα-depleted medium was immunoblotted with the anti-APP-N-terminal antibody (for sAPPβ) and with 6E10 (for the confirmation of sAPPα depletion). Intracellular C99 in RIPA-solubilized lysates (1.5 mg) was immunoprecipitated with BAN50 and immunodetected with B12/4 as previously described (Sai *et al.* 2002). Intracellular C83 in RIPA-solubilized lysates (1.5 mg) was immunodetected with the antibody against the APP C-terminal fragment 369. Data are representative of three independent experiments.

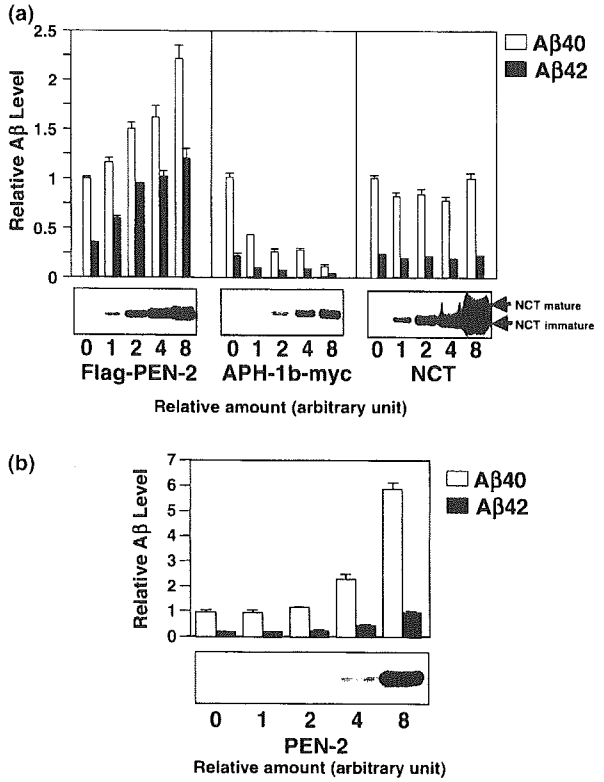

Fig. 2 Effect of various levels of PEN-2, APH-1b or nicastrin (NCT) on amyloid β-protein (Aβ) generation. (a) After PEN-2, APH-1b or NCT was retrovirally expressed in fibroblasts (2×10^5) expressing β-amyloid precursor protein (APP)695 (presenilin, endogenous levels), Aβ40 and Aβ42 secreted from cells during a 48-h culture were quantified by ELISA. The Aβ levels were normalized to soluble APP and then expressed as relative to basal Aβ40 levels obtained from mock-transfected cells as described in (a). Numbers used for arbitrary units denote the relative concentration of the virus solution containing pMX carrying the indicated cDNA used for the infection (the concentration of the original virus solution is defined as 8 arbitrary units). Values are means ± SD of two independent dishes ($n = 2$). The RIPA-solubilized lysates (10 μg) were immunoblotted with the anti-FLAG antibody (for PEN-2), anti-myc antibody (for APH-1b) or anti-NCT antibody. FLAG-PEN-2, N-terminally FLAG-tagged PEN-2; APH-1b-myc, C-terminally myc-tagged APH-1b. Data are representative of four independent experiments. (b) PEN-2 without the FLAG tag was also retrovirally expressed and secreted Aβ was quantified as described in (a). The RIPA-solubilized lysates (10 μg) were immunoblotted with the anti-PEN-2 antibody.

PS1 NTF and CTF. Figure 3(c) demonstrates that no drastic increase in γ-secretase activity was observed with various expression levels of NTF or CTF. In this experiment, it appears that γ-secretase activity is saturable at the minimum expression levels of NTF and CTF. Therefore, we next determined the effect of the expression of PS cofactors on Aβ generation mediated by the coexpression of PS1 NTF and CTF at the expression level at which Aβ increase is saturated.

Effect of expression of presenilin cofactors on amyloid β-protein generation mediated by the coexpression of N- and C-terminal fragments in presenilin-null cells

As shown in Figs 4(a) and (b), only PEN-2 expression significantly increased Aβ generation mediated by the coexpression of PS1 NTF/CTF, while the expression of NCT or APH-1 alone did not cause a significant increase in Aβ generation. Interestingly, the levels of PS1 NTF and CTF were greatly increased by the coexpression of NCT and APH-1b, accompanied by the stimulation of NCT maturation as observed in cells expressing the PS1 holoprotein with all of the cofactors (Fig. 4b). Therefore, it appears that PS1 NTF and CTF are stabilized by the binding of both APH-1 and NCT to PS1 NTF and CTF. Moreover, it was noted that the expression of PEN-2 together with the expression of APH-1b and NCT further stimulated NCT maturation. However, it was noted that the increase in Aβ generation by PEN-2 expression was not associated with the stimulation of NCT maturation or the increase in the levels of PS1 NTF and CTF. It was also noted that the expression of APH-1b clearly inhibited the PEN-2-mediated increase in Aβ generation.

We next investigated whether the inhibitory effect of APH-1b on the PEN-2-mediated increase in Aβ generation results from the inhibition of the binding of PEN-2 to PS due to APH-1b expression. For this purpose, we investigated whether the level of PEN-2 bound to PS1 changes with an increase in the expression level of APH-1b (Fig. 4c). APH-1b did not inhibit the binding of PEN-2 to PS1 (Fig. 4c). In contrast, an increase in the level of APH-1b bound to PS1 caused an increase in the level of PEN-2 bound to PS1 (Fig. 4c, lower panel), although Aβ generation decreased with an increase in the expression level of APH-1b (Fig. 4c, upper panel). We also observed that APH-1b did not inhibit the binding of NCT to PS1 (Fig. 4c, lower panel). This result indicates that the inhibition of the PEN-2-mediated increase in Aβ generation by APH-1b is not due to the inhibition of the binding of PEN-2 to PS1.

PEN-2 does not enhance presenilin 1 heterodimer formation

The PS NTF/CTF heterodimers are considered to constitute the active site in the γ-secretase complex (Esler *et al.* 2000; Li *et al.* 2000b). Therefore, PEN-2 could stimulate PS1 NTF/CTF heterodimer formation in PS-null cells coexpressing PS1 NTF and CTF because PEN-2 increases Aβ generation. To test this possibility, we first determined whether PS1 NTF and CTF coexpressed in PS-null cells form the PS1 NTF/CTF heterodimer. The anti-PS1 NTF antibody coimmunoprecipitated PS1 CTF and the anti-PS1 CTF antibody also coimmunoprecipitated PS1 NTF (Fig. 5a). This result clearly indicates that PS1 NTF and CTF form the PS1 NTF/CTF heterodimer complex in PS-null cells. However, PEN-2 did not stimulate the formation of the heterodimer (Fig. 5a). We also examined the effect of PEN-2 expression on PS

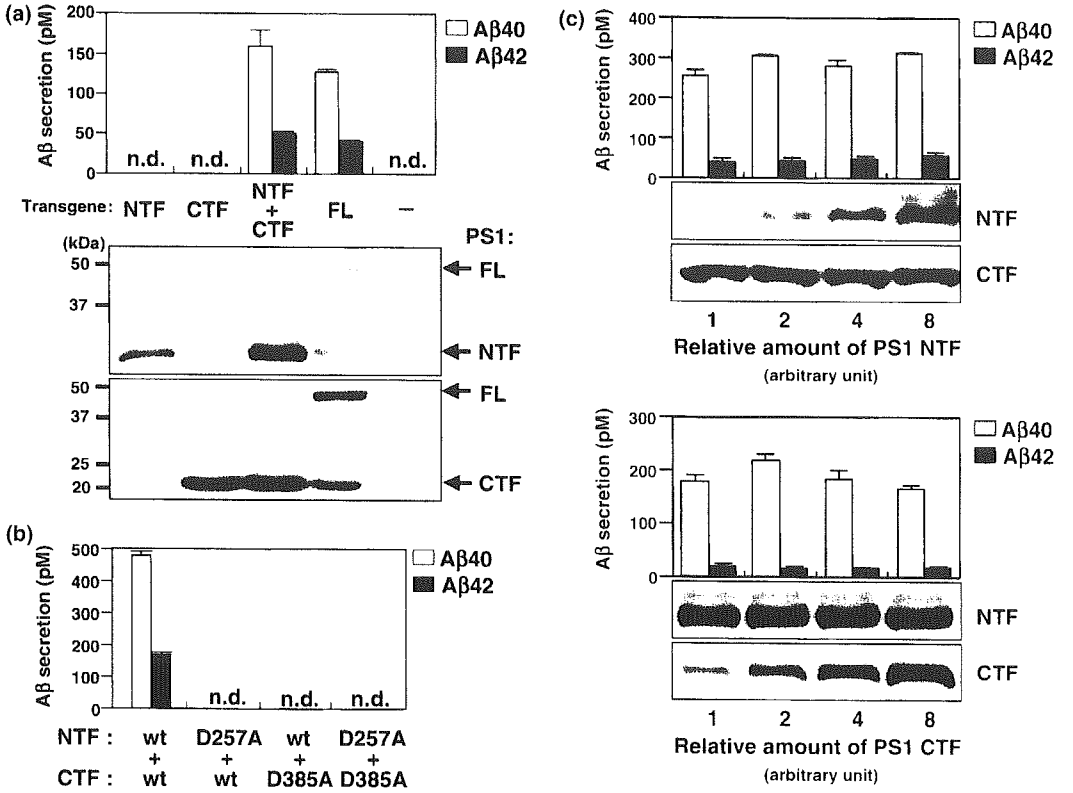

Fig. 3 Coexpression of presenilin (PS)1 N- and C-terminal fragments (NTF and CTF) restores amyloid β-protein (Aβ) generation in PS-null cells. (a) The indicated exogenous cDNAs and β-amyloid precursor protein (APP)695 were retrovirally expressed in PS-null cells. The Aβ40 and Aβ42 secreted from cells during a 48-h culture were quantified by ELISA. Ristocetin-induced platelet agglutination-solubilized lysates (10 μg) were immunoblotted with the anti-PS1 NTF antibody (for PS1 NTF detection) or anti-PS1 loop antibody (for PS1 CTF detection). FL, PS1 full-length; n.d., Aβ was not detected (< 10 pM). (b) Coexpression of PS1 NTF mutated at Asp257 and CTF or PS1 NTF and CTF mutated at Asp285 does not restore Aβ generation in PS-null cells. wt, wild-type PS1. (c) Effects of various expression levels of PS1 NTF and CTF on Aβ generation in PS-null cells. In the upper panel, using various concentrations (arbitrary units 1–8) of the virus solution containing PS1 NTF cDNA and a constant concentration (8 arbitrary units) of the virus solution containing PS1 CTF cDNA, PS1 NTF and CTF were retrovirally expressed in PS-null cells (2×10^5) expressing APP695. In the lower panel, using various concentrations (arbitrary units 1–8) of the virus solution containing PS1 CTF cDNA and a constant concentration (8 arbitrary units) of the virus solution containing PS1 NTF cDNA, PS1 NTF and CTF were retrovirally expressed in PS-null cells (2×10^5) expressing APP695. The Aβ40 and Aβ42 secreted from cells during a 48-h culture were quantified by ELISA. Note: as far as the concentration of the viral solution showing 100% infection efficiency was used, a decrease in Aβ generation was not observed, although the expression of NTF alone or CTF alone resulted in no detectable Aβ generation.

NTF/NTF dimer formation in PS-null cells coexpressing N-terminal HA-tagged PS1 NTF and wild-type PS1 NTF/CTF because it was previously reported that PS is likely to form NTF/NTF dimers (Schroeter *et al.* 2003). However, we failed to detect a PS1 NTF/NTF dimer even when we employed N-terminal HA-tagged PS1 holoprotein and PEN-2 did not enhance the formation of NTF/NTF dimer (data not shown).

PEN-2 interaction with N- and C-terminal fragments

To understand the mechanism underlying the increase in Aβ generation by PEN-2, as an initial step we determined which fragment, NTF or CTF, interacts with PEN-2. The anti-PS1 NTF antibody clearly coimmunoprecipitated PEN-2 and the anti-PS1 CTF antibody also coimmunoprecipitated PEN-2 (Fig. 5b, upper panel). The anti-FLAG antibody also coimmunorecipitated PS1 NTF and CTF (Fig. 5b, lower panel). Thus, our results show that PEN-2 binds to both NTF and CTF.

Effect of γ-secretase inhibitors on PEN-2-mediated increase in amyloid β-protein generation in presenilin-null cells coexpressing presenilin 1 N- and C-terminal fragments

To address the mechanism underlying the increase in Aβ generation by PEN-2 expression, we finally investigated whether PEN-2 expression alters the IC_{50} of a specific inhibitor of γ-secretase, L-685,458, which was previously

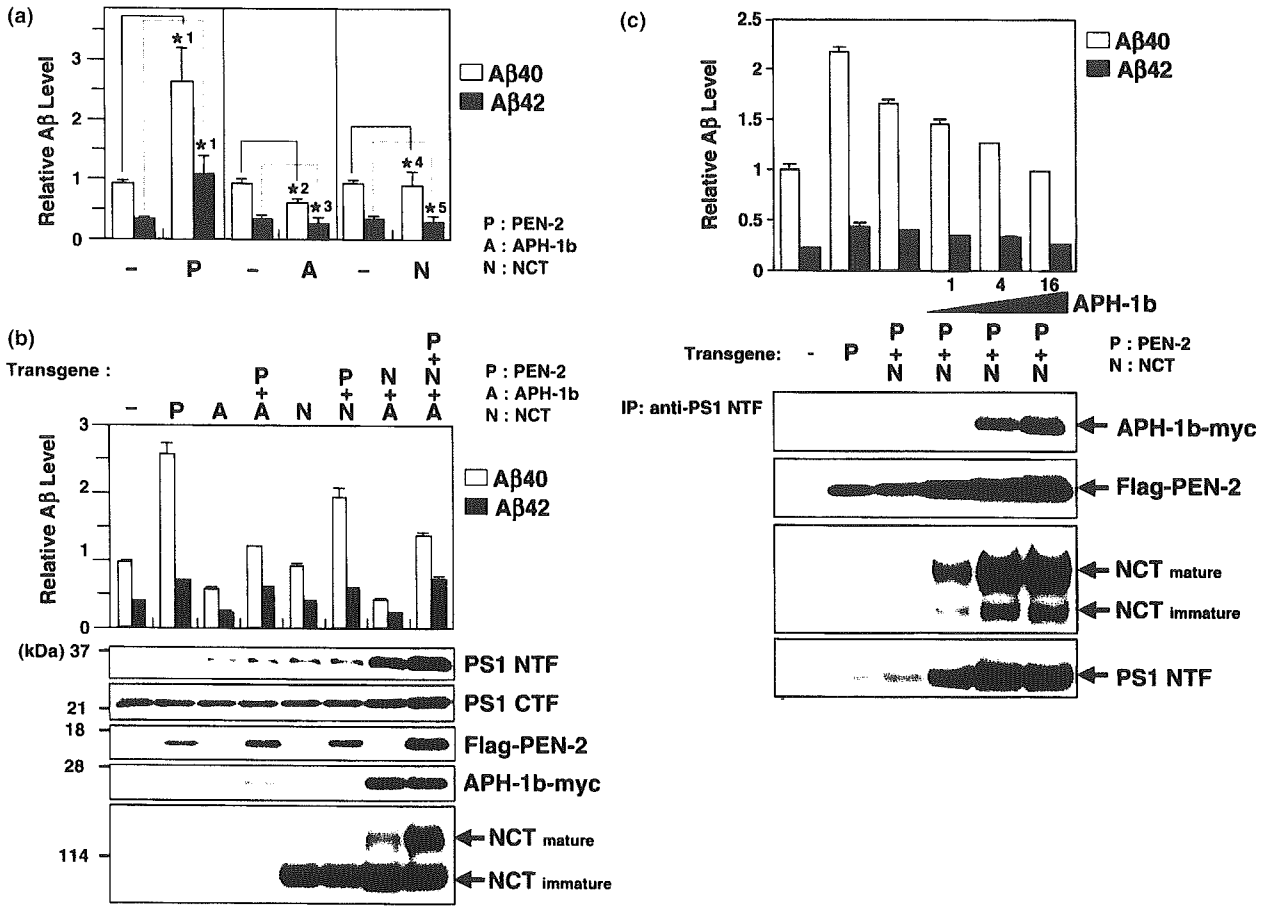

Fig. 4 Effects of expression of PEN-2, APH-1b and/or nicastrin (NCT) on amyloid β-protein (Aβ) generation in presenilin (PS)-null cells coexpressing PS1 N-/C-terminal fragment (NTF/CTF). (a) The indicated exogenous genes were retrovirally expressed in PS-null cells coexpressing PS1 NTF/CTF and expressing β-amyloid precursor protein (APP)695. The Aβ40 and Aβ42 secreted from 48-h cultured cells were quantified by ELISA. The Aβ levels were expressed as relative to basal Aβ40 levels obtained from PS-null cells expressing PS1 NTF and CTF. –, mock infection (retroviral vector, pMX, alone). P, FLAG-PEN-2; A, APH-1b-myc; N, NCT. Significant difference at $^{*1}p < 0.0001$ ($n = 16$), $^{*2}p < 0.001$ ($n = 8$), $^{*3}p < 0.05$ ($n = 8$), $^{*4}p > 0.5$ ($n = 10$) and $^{*5}p > 0.5$ ($n = 10$). (b) The indicated exogenous genes were retrovirally expressed in PS-null cells coexpressing PS1 NTF/CTF and expressing APP695. Values are means ± SD of two independent dishes ($n = 2$). The Aβ levels normalized to soluble APP were expressed as relative to basal Aβ40 levels obtained from PS-null cells expressing PS1 NTF and CTF as described in (a). Similar results were obtained from three independent experiments. The RIPA-solubilized lysates (10 μg) were immunoblotted with the anti-PS1 NTF antibody, anti-PS1 loop antibody, anti-NCT antibody, anti-FLAG antibody (for FLAG-tagged PEN-2) and anti-myc antibody (for myc-tagged APH-1b). Note that the long exposure revealed endogenous NCT in the first four lanes (data not shown). (c) APH-1b expression inhibits the PEN-2-induced enhancement of Aβ generation in PS-null cells coexpressing PS1 NTF and CTF. In the upper panel, the indicated exogenous genes were retrovirally expressed in PS-null cells coexpressing PS1 NTF/CTF and APP695. Using various concentrations of the virus solution containing APH-1b-myc cDNA (arbitrary units 1–16), APH-1b-myc was expressed at various levels. P, FLAG-PEN-2; A, APH-1b-myc; N, NCT. Note: the same results showing that APH-1b inhibits the PEN-2-mediated increase in Aβ generation were obtained from four independent experiments. In the lower panel, CHAPSO-solubilized lysates (1 mg) in the upper panel were immunoprecipitated (IP) with the anti-PS1 NTF antibody and then immunoblotted with the anti-myc antibody (for myc-tagged APH-1b), anti-FLAG antibody (for FLAG-tagged PEN-2), anti-NCT antibody or anti-PS1 NTF antibody.

characterized as a transition state analogue mimic at the catalytic site of an aspartyl protease (Shearman *et al.* 2000). It was also shown that the structurally related photoaffinity analogues of L-685,458 exclusively bind to PS NTF and CTF (Li *et al.* 2000b). As shown in Fig. 6(a), PEN-2 expression significantly reduced IC_{50} against Aβ formation compared with mock-transfected cells. In addition, we found that PEN-2 expression also reduced the IC_{50} of a non-transition state analogue inhibitor, DAPT (Dovey *et al.* 2001) (Fig. 6b), which was suggested to either directly bind

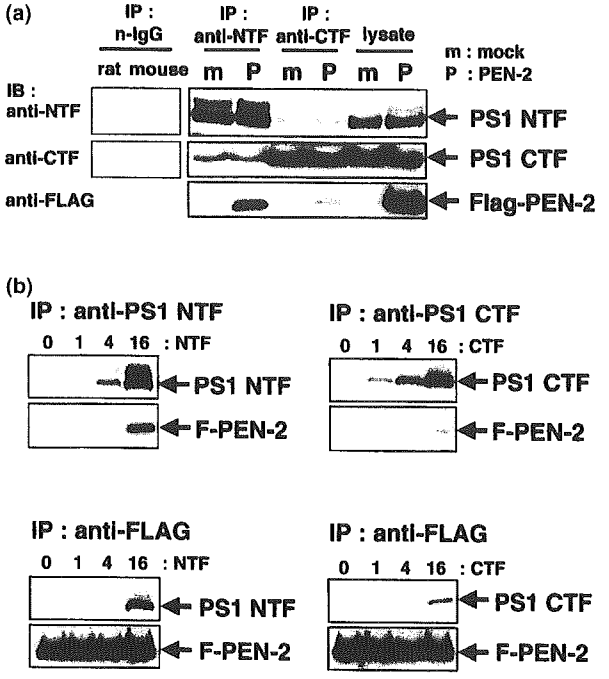

Fig. 5 Effect of PEN-2 expression on (a) presenilin (PS)1 N-/C-terminal fragment (NTF/CTF) heterodimer formation and (b) the interaction of PEN-2 with PS1 NTF and CTF. (a) CHAPSO-solubilized lysates (1 mg) from PS-null cells coexpressing PS1 NTF/CTF were immunoprecipitated (IP) with the anti-PS1 NTF antibody and then immunoblotted (IB) with the anti-PS1 NTF antibody, anti-PS1 loop antibody or anti-FLAG antibody (right panel, left two lanes). The same lysates were IP with the anti-PS1 loop antibody and then IB with the indicated antibodies (right panel, middle two lanes). The same lysates (10 μg) without immunoprecipitation were also IB with the indicated antibodies (right panel, right two lanes). In the left panel, the same lysates were IP with rabbit normal IgG (control for the anti-PS1 NTF antibody) or mouse normal IgG (control for the anti-PS1 loop antibody) and then IB with the anti-PS1 NTF antibody and anti-PS1 loop antibody. Note: the anti-PS1 loop antibody used in this study immunoprecipitates PS1 CTF but not PS1 NTF (data not shown). (b) In the upper two panels, a constant level of FLAG-PEN-2 and various levels (arbitrary units 0–16) of PS1 NTF (left panel) or CTF (right panel) were retrovirally expressed in PS-null cells. CHAPSO-solubilized lysates (1 mg) were IP with the anti-PS1 antibody (left panel) or anti-PS1 loop antibody (right panel). The immunoprecipitation products were then IB with the anti-FLAG antibody and anti-PS1 antibody (left panel) or the anti-PS1 loop antibody (right panel). In the lower two panels, the same lysates (1 mg) were IP with the anti-FLAG antibody. The immunoprecipitation products were then IB with the anti-FLAG antibody and anti-PS1 antibody (left panel) or the anti-PS1 loop antibody (right panel). F-PEN-2, FLAG-PEN-2.

to the active site or alter it through an allosteric effect because these inhibitors prevent PS labelling with a transition state analogue affinity reagent (Kornilova *et al.* 2003). These results suggest that the expression of PEN enhances the direct affinity or the accessibility of the γ-secretase substrate to the catalytic site (see Discussion). Similar reductions in the

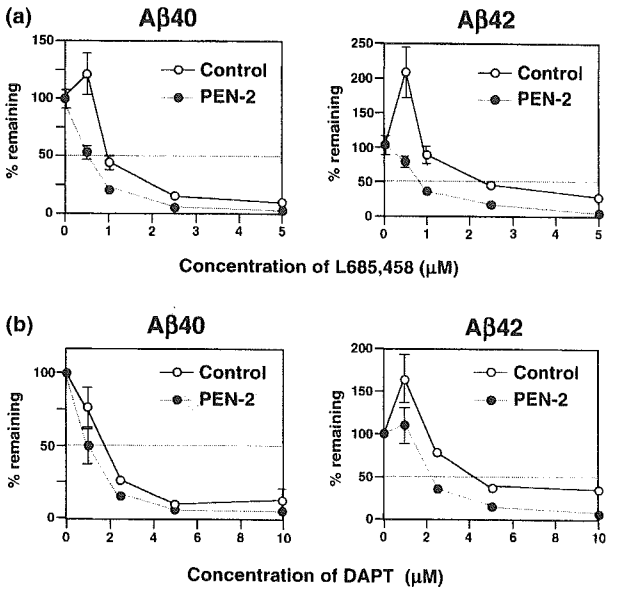

Fig. 6 Effects of γ-secretase inhibitors on PEN-2-mediated increase in amyloid β-protein (Aβ) generation in presenilin (PS)-null cells coexpressing PS1 N- and C-terminal fragments (NTF and CTF). Seventy-two hours after PS1 NTF/CTF and PEN-2 or mock was retrovirally coexpressed in PS-null cells (2×10^5) stably expressing APP695, the cells were treated with the indicated concentrations of (a) a transition state analogue, L-685,458, and (b) a non-transition state analogue, DAPT, in a fresh medium and incubated for 24 h. The Aβ40 and Aβ42 secreted from 24-h-cultured cells were quantified by ELISA. Data are expressed as a percentage of the mean Aβ level of untreated controls (vehicle-treated cells). ○, mock infection; ●, cells retrovirally expressing exogenous FLAG-PEN-2. Values are means ± SD of four independent dishes ($n = 4$). The IC_{50} of the inhibitors was as follows: L-685,458 (PEN-2 expression, mock expression), Aβ40 (0.5 μM, 1 μM), Aβ42 (0.8 μM, 2.2 μM); DAPT, Aβ40 (1 μM, 1.6 μM), Aβ42 (2 μM, 4 μM).

IC_{50} of another transition state analogue inhibitor, WPE-III-31C (Esler *et al.* 2002), and another non-transition state analogue inhibitor, Compound E (Seiffert *et al.* 2000), were observed [IC_{50} of WPE-III-31C (PEN-2 expression, mock expression): Aβ40 (2 μM, 8 μM), Aβ42 (1.8 μM, 2.2 μM); Compound E: Aβ40 (0.5 nM, 0.8 nM), Aβ42 (2 nM, 7 nM)].

Discussion

It was previously shown that NCT, APH-1 and PEN-2 constitute the essential components of the functional PS complex (Francis *et al.* 2002; Lee *et al.* 2002; Steiner *et al.* 2002; Edbauer *et al.* 2003; Hu and Fortini 2003; Kim *et al.* 2003; Kimberly *et al.* 2003; Luo *et al.* 2003; Takasugi *et al.* 2003). Although it has been firmly established that the formation of the active γ-secretase requires all four components, PS, PEN-2, NCT and APH-1, the precise individual roles of the three cofactors with regard to Aβ generation are unclear because it is not known whether the cofactors are only necessary for PS endoproteolysis and the formation of the active γ-secretase or

whether they also play a role in Aβ generation after the formation of the γ-secretase complex. Our study, using a retrovirus expression system, of the effects of various expression levels of the three cofactors on Aβ generation clearly demonstrated that exogenous PEN-2 expression increases Aβ generation. However, this result was discrepant from earlier works showing that an enhanced γ-secretase activity was observed when all four components (PS, NCT, APH and PEN-2) are expressed using the stable transfectant (Kimberly *et al.* 2003; Takasugi *et al.* 2003). Although, at present, the exact reason for this discrepancy is not known, one possible explanation is that it is caused by the difference in exogenous PEN-2 level in the cells expressing PEN-2 alone between our study and other studies. As the intracellular levels of PEN-2 and APH-1 are tightly regulated, as previously reported (Gu *et al.* 2002; Lee *et al.* 2002; Steiner *et al.* 2002; Bergman *et al.* 2004; Crystal *et al.* 2004; Prokop *et al.* 2004), it will be difficult to obtain cells stably expressing PEN-2 or APH-1 at a high level because their intracellular levels could be under this tight regulation during a drug selection step for obtaining a stable transfectant. Indeed, in the earlier works, the PEN-2 level in cells stably expressing PEN-2 alone was definitely lower than that in cells expressing all four components (Kimberly *et al.* 2003; Takasugi *et al.* 2003). As suggested in our study (Fig. 4b), PEN-2 appears to be greatly stabilized when the other three components are coexpressed. Therefore, it will be difficult to compare the effect of PEN-2 on Aβ generation between PEN-2-expressing cells and three-cofactor-coexpressing cells when the PEN-2 expression level is different between them. The retroviral gene transfer system used in this study efficiently delivers gene stably into a target cell without drug selection during a short time. It allows the induction of a stable PEN-2 expression at a high level similar to that observed in three-cofactor-coexpressing cells and comparison between the effect of the expression of PEN-2 alone and that of the coexpression of PEN-2 with the other cofactors (Fig. 1a). Although we cannot completely exclude the unknown indirect effect of the overexpression of these cofactors, our present results strongly suggest that the level of PEN-2 or APH-1 affects γ-secretase activity even after PS endoproteolysis occurs.

Therefore, we next investigated whether γ-secretase activity can be reconstituted by the coexpression of PS NTF and CTF in PS-null cells, as the study of the coexpression of PS NTF and CTF in PS-null cells allows us to distinguish the roles of the cofactors in Aβ generation from the roles in PS endoproteolysis. Previously, it was shown that the coexpression of PS1 NTF and CTF rescues the *sel-12* egg-laying defect, suggesting that the coexpression of PS1 and CTF induces biologically active PS in the cells (Levitan *et al.* 2001). That study also showed that the coexpression of PS NTF and CTF in HEK293 cells does not further increase γ-secretase activity, suggesting that the coexpression of NTF and CTF does not reconstitute γ-secretase activity (Levitan *et al.* 2001). However, we assumed that this result only suggests that γ-secretase activity is saturable, instead of the coexpression of NTF and CTF failing to form the functional complex for γ-secretase activity in cells. Indeed, in the present study, we demonstrated that the coexpression of NTF and CTF induces γ-secretase activity similarly to the PS holoprotein in PS-null cells. In addition, our present study of the reconstitution of γ-secretase activity by NTF/CTF coexpression demonstrated that Asp257 or Asp385 in PS is required for γ-secretase activity. It was also noted that, in this reconstitution of γ-secretase activity in PS-null cells, γ-secretase activity is saturable at certain expression levels of NTF and CTF as observed in cells expressing the PS holoprotein.

In the reconstitution of γ-secretase activity by the coexpression of PS NTF and CTF in PS-null cells, we noted that PEN-2 expression increases Aβ generation but APH-1b expression has an inhibitory effect on PEN-2 stimulation of Aβ generation without inhibiting the binding of PEN-2 to PS. It was also noted that the coexpression of all cofactors in PS-null cells expressing PS1 NTF/CTF does not increase Aβ generation similarly to full-length PS (Figs 1a and b and 4b and c). A possible explanation for this is as follows. The binding of NCT and APH-1 (and PEN-2) to full-length PS is suggested to be a prerequisite of the formation of an active γ-secretase from full-length PS (Hu and Fortini 2003; LaVoie *et al.* 2003; Takasugi *et al.* 2003). However, in the reconstitution of γ-secretase by the coexpression of PS NTF and CTF, the situation may be slightly different because there is no full-length PS in PS-null cells. Therefore, the absence of the step prerequisite to the assembly of cofactors with full-length PS can lead to a smaller effect of all the coexpressed cofactors on γ-secretase activity restored by the expression of PS NTF/CTF than those on γ-secretase activity observed in full-length PS-expressing cells. Our results strongly suggest that the molecular ratio of APH-1 to PEN-2 bound to PS is critical for determining the degree of γ-secretase activity after the formation of a heterodimer complex.

Interestingly, the coexpression of APH-1, PEN-2 and NCT greatly stabilizes the expression levels of PS1 NTF and CTF, accompanied by the stimulation of NCT maturation. However, the stimulation of NCT maturation is not associated with the enhancement of Aβ generation. Recently, it has been shown that the expression of PS1 with a mutation at Asp257 or Asp385 also hastens NCT maturation, indicating that PS catalytic activity is separable from the transport of a γ-secretase complex (Nyabi *et al.* 2003). Our present data also agree with this interpretation. In addition, our study demonstrated that the enhancement of Aβ generation by PEN-2 expression is not associated with the increase in the level of PS1 NTF/CTF. Recent studies have strongly suggested that only a small portion of the PS complex is

involved in an active γ-secretase complex (Lai *et al.* 2003; Gu *et al.* 2004). Therefore, after the formation of an active γ-secretase complex, the activity could be regulated by losing the cofactor(s) from the PS complex or by further binding the cofactor(s) to the PS complex.

To address the mechanism underlying the increase in Aβ generation by PEN-2 expression, we investigated whether PEN-2 expression enhances the formation of PS1 NTF/CTF heterodimers in PS-null cells because PS NTF/CTF heterodimers are believed to constitute the active site in the γ-secretase complex (Esler *et al.* 2000; Li *et al.* 2000b). We found that PEN-2 expression does not enhance PS1 NTF/CTF heterodimer formation, probably because PEN-2 appears not to equivalently interact with both PS1 fragments (Fraering *et al.* 2004). At present, the precise mechanism underlying the increase in Aβ generation by PEN-2 expression has not been elucidated. However, PEN-2 expression caused a significant reduction in the IC_{50} of a transition state analogue γ-secretase inhibitor for Aβ generation, suggesting that PEN-2 expression enhances the direct affinity or the accessibility of the transition state analogue to the catalytic site. PEN-2 expression also reduced the IC_{50} of the non-transition state analogue inhibitors, which were suggested to act at partially overlapping sites where the transition state analogue inhibitors act because these inhibitors prevent PS labelling with a transition state analogue affinity reagent (Kornilova *et al.* 2003). Therefore, it is likely that PEN-2 expression enhances the direct affinity or the accessibility of these non-transition state analogue inhibitors to the overlapping sites where the transition state analogue acts. Although more precise studies using the inhibitors are required, we can speculate that the binding of PEN-2 to PS may enhance the direct affinity or the accessibility of the γ-secretase substrate to the catalytic site, resulting in an increase in γ-secretase activity.

Our present study strongly suggests that PEN-2 is not only a component of the functional PS complex but is also an enhancer of PS-mediated γ-cleavage after PS heterodimer formation. Our results also raise the possibility that PEN-2 regulates γ-secretase activity positively and APH-1 negatively after the functional PS complex is formed. Further studies on how PEN-2 and APH-1 regulate γ-secretase activity using an *in vitro* system will help clarify the molecular mechanism underlying PS-mediated γ-secretase activity.

Acknowledgements

This study was supported by a research grant for Longevity Sciences; Brain Science Research from the Ministry of Health, Labor and Welfare, Japan and the Program for Promotion of Fundamental Studies in Health Sciences of the Organization for Pharmaceutical Safety and Research. We thank B. De Strooper (Katholieke Universiteit Leuven and Flanders Interuniversity Heveatraat, Belgium) for the supply of antibody B12/4, PS1/PS2 double-deficient fibroblasts and wild-type fibroblasts and S. Gandy for providing antibody 369.

Note added in proof

While this manuscript was being revised, a study on the coexpression of PS1 NTF and CTF in PS-null cells was published (Laudon *et al.* 2004). The authors showed that the coexpression of PS1 NTF and CTF restored γ-secretase activity similar to our results; however, the effects of PS cofactors on Aβ generation restored by the coexpression of NTF/CTF in PS-null cells were not examined in their study.

References

Asami-Odaka A., Ishibashi Y., Kikuchi T., Kitada C. and Suzuki N. (1995) Long amyloid β-protein secreted from wild-type human neuroblastoma IMR-32 cells. *Biochemistry* **34**, 10272–10278.

Bergman A., Hansson E. M., Pursglove S. E., Farmery M. R., Lannfelt L., Lendahl U., Lundkvist J. and Naslund J. (2004) Pen-2 is sequestered in the endoplasmic reticulum and subjected to ubiquitylation and proteasome-mediated degradation in the absence of presenilin. *J. Biol. Chem.* **279**, 16744–16753.

Buxbaum J. D., Gandy S. E., Cicchetti P., Ehrlich M. E., Czernik A. J., Fracasso R. P., Ramabhadran T. V., Unterbeck A. J. and Greengard P. (1990) Processing of Alzheimer β/A4 amyloid precursor protein: modulation by agents that regulate protein phosphorylation. *Proc. Natl Acad. Sci. USA* **87**, 6003–6006.

Crystal A. S., Morais V. A., Fortna R. R., Carlin D., Pierson T. C., Wilson C. A., Lee V. M. and Doms R. W. (2004) Presenilin modulates Pen-2 levels posttranslationally by protecting it from proteasomal degradation. *Biochemistry* **43**, 3555–3563.

De Strooper B., Simons M., Multhaup G., Van Leuven F., Beyreuther K. and Dotti C. G. (1995) Production of intracellular amyloid-containing fragments in hippocampal neurons expressing human amyloid precursor protein and protection against amyloidogenesis by subtle amino acid substitutions in the rodent sequence. *EMBO J.* **14**, 4932–4938.

De Strooper B., Saftig P., Craessaerts K., Vanderstichele H., Guhde G., Annaert W., Von Figura K. and Van Leuven F. (1998) Deficiency of presenilin-1 inhibits the normal cleavage of amyloid precursor protein. *Nature* **391**, 387–390.

De Strooper B., Annaert W., Cupers P. *et al.* (1999) A presenilin-1-dependent γ-secretase-like protease mediates release of Notch intracellular domain. *Nature* **398**, 518–522.

Dovey H. F., John V., Anderson J. P. *et al.* (2001) Functional gamma-secretase inhibitors reduce beta-amyloid peptide levels in brain. *J. Neurochem.* **76**, 173–181.

Edbauer D., Winkler E., Haass C. and Steiner H. (2002) Presenilin and nicastrin regulate each other and determine amyloid β-peptide production via complex formation. *Proc. Natl Acad. Sci. USA* **99**, 8666–8671.

Edbauer D., Winkler E., Regula J. T., Pesold B., Steiner H. and Haass C. (2003) Reconstitution of γ-secretase activity. *Nat. Cell Biol.* **5**, 486–488.

Esler W. P., Kimberly W. T., Ostaszewski B. L., Diehl T. S., Moore C. L., Tsai J. Y., Rahmati T., Xia W., Selkoe D. J. and Wolfe M. S. (2000) Transition-state analogue inhibitors of γ-secretase bind directly to presenilin-1. *Nat. Cell Biol.* **2**, 428–434.

Esler W. P., Kimberly W. T., Ostaszewski B. L., Ye W., Diehl T. S., Selkoe D. J. and Wolfe M. S. (2002) Activity-dependent isolation

of the presenilin-gamma-secretase complex reveals nicastrin and a γ substrate. *Proc. Natl Acad. Sci. USA* **99**, 2720–2725.

Fraering P. C., LaVoie M. J., Ye W., Ostaszewski B. L., Kimberly W. T., Selkoe D. J. and Wolfe M. S. (2004) Detergent-dependent dissociation of active γ-secretase reveals an interaction between Pen-2 and PS1-NTF and offers a model for subunit organization within the complex. *Biochemistry* **43**, 323–333.

Francis R., McGrath G., Zhang J. *et al.* (2002) aph-1 and pen-2 are required for Notch pathway signaling, γ-secretase cleavage of βAPP, and presenilin protein accumulation. *Dev. Cell* **3**, 85–97.

Goutte C., Tsunozaki M., Hale V. A. and Priess J. R. (2002) APH-1 is a multipass membrane protein essential for the Notch signaling pathway in Caenorhabditis elegans embryos. *Proc. Natl Acad. Sci. USA* **99**, 775–779.

Gu Y., Misonou H., Sato T., Dohmae N., Takio K. and Ihara Y. (2001) Distinct intramembrane cleavage of the β-amyloid precursor protein family resembling γ-secretase-like cleavage of Notch. *J. Biol. Chem.* **276**, 35 235–35 238.

Gu Y., Chen F., Sanjo N. *et al.* (2002) APH-1 interacts with mature and immature forms of presenilins and nicastrin and may play a role in maturation of presenilin-nicastrin complexes. *J. Biol. Chem.* **278**, 7374–7854.

Gu Y., Sanjo N., Chen F. *et al.* (2004) The presenilin proteins are components of multiple membrane-bound complex which have different biological activities. *J. Biol. Chem.* in press.

Herreman A., Serneels L., Annaert W., Collen D., Schoonjans L. and De Strooper B. (2000) Total inactivation of γ-secretase activity in presenilin-deficient embryonic stem cells. *Nat. Cell Biol.* **2**, 461–462.

Hu Y. and Fortini M. E. (2003) Different cofactor activities in gamma-secretase assembly: evidence for a nicastrin-Aph-1 subcomplex. *J. Cell Biol.* **161**, 685–690.

Kim S. H., Ikeuchi T., Yu C. and Sisodia S. S. (2003) Regulated hyperaccumulation of presenilin-1 and the 'γ-secretase' complex. Evidence for differential intramembranous processing of transmembrane subatrates. *J. Biol. Chem.* **278**, 33 992–34 002.

Kimberly W. T., LaVoie M. J., Ostaszewski B. L., Ye W., Wolfe M. S. and Selkoe D. J. (2003) γ-Secretase is a membrane protein complex comprised of presenilin, nicastrin, Aph-1, and Pen-2. *Proc. Natl Acad. Sci. USA* **100**, 6382–6387.

Komano H., Shiraishi H., Kawamura Y., Sai X., Suzuki R., Serneels L., Kawaichi M., Kitamura T. and Yanagisawa K. (2002) A new functional screening system for identification of regulators for the generation of amyloid beta-protein. *J. Biol. Chem.* **277**, 39 627–39 633.

Kornilova A. Y., Das C. and Wolfe M. S. (2003) Differential effects of inhibitors on the γ-secretase complex. Mechanistic implications. *J. Biol. Chem.* **278**, 16 470–16 473.

Lai M. T., Chen E., Crouthamel M. C. *et al.* (2003) Presenilin-1 and presenilin-2 exhibit distinct yet overlapping gamma-secretase activities. *J. Biol. Chem.* **278**, 22 475–22 481.

Lammich S., Okochi M., Takeda M., Kaether C., Capell A., Zimmer A. K., Edbauer D., Walter J., Steiner H. and Haass C. (2002) Presenilin-dependent intramembrane proteolysis of CD44 leads to the liberation of its intracellular domain and the secretion of an Abeta-like peptide. *J. Biol. Chem.* **277**, 44 754–44 759.

Laudon H., Mathews P. M., Karlstrom H. *et al.* (2004) Co-expressed presenilin 1 NTF and CTF form functional γ-secretase complexes in cells devoid of full-length protein. *J. Neurochem.* **89**, 44–53.

LaVoie M. J., Fraering P. C., Ostaszewski B. L., Ye W., Kimberly W. T., Wolfe M. S. and Selkoe D. J. (2003) Assembly of the γ-secretase complex involves early formation of an intermediate subcomplex of Aph-1 and nicastrin. *J. Biol. Chem.* **278**, 37 213–37 222.

Lee H. J., Jung K.M., Huang Y.Z , Bennet L.B , Lee J.S., Mei L. and Kim T.W. (2002) Presenilin-dependent γ-secretase-like intramembrane cleavage of ErbB4. *J. Biol. Chem.* **277**, 6318–6323.

Lee S. F., Shah S., Li H., Yu C., Han W. and Yu G. (2002) Mammalian APH-1 interacts with presenilin and nicastrin and is required for intramembrane proteolysis of amyloid-β precursor protein and notch. *J. Biol. Chem.* **277**, 45 013–45 019.

Levitan D., Lee J., Song L., Manning R., Wong G., Parker E. and Zhang L. (2001) PS1 N- and C-terminal fragments form a complex that functions in APP processing and Notch signaling. *Proc. Natl Acad. Sci. USA* **98**, 12 186–12 190.

Li Y. M., Lai M. T., Xu M., Huang Q., DiMuzio-Mower J., Sardana M. K., Shi X. P., Yin K. C., Shafer J. A. and Gardell S. J. (2000a) Presenilin 1 is linked with γ-secretase activity in the detergent solubilized state. *Proc. Natl Acad. Sci. USA* **97**, 6138–6143.

Li Y. M., Xu M., Lai M. T. *et al.* (2000b) Photoactivated γ-secretase inhibitors directed to the active site covalently label presenilin 1. *Nature* **405**, 689–694.

Luo W. J., Wang H., Li H., Kim B. S., Shah S., Lee H. J., Thinakaran G., Kim T. W., Yu G. and Xu H. (2003) PEN-2 and APH-1 coordinately regulate proteolytic processing of presenilin 1. *J. Biol. Chem.* **278**, 7850–7854.

Marambaud P., Shioi J., Serban G. *et al.* (2002) A presenilin-1/γ-secretase cleavage releases the E-cadherin intracellular domain and regulates disassembly of adherens junctions. *EMBO J.* **21**, 1948–1956.

Marambaud P., Wen P. H., Dutt A., Shioi J., Takashima A., Siman R. and Robakis N. K. (2003) A CBP binding transcriptional repressor produced by the PS1/epsilon-cleavage of N-cadherin is inhibited by PS1 FAD mutations. *Cell* **114**, 635–645.

Murakami D., Okamoto I., Nagano O., Kawano Y., Tomita T., Iwatsubo T., De Strooper B., Yumoto E. and Saya H. (2003) Presenilin-dependent γ-secretase activity mediates the intramembranous cleavage of CD44. *Oncogene* **22**, 1511–1516.

Ni C. Y., Murphy M. P., Golde T. E. and Carpenter G. (2001) γ-Secretase cleavage and nuclear localization of ErbB-4 receptor tyrosine kinase. *Science* **294**, 2179–2181.

Nyabi O., Bentahir M., Horre K., Herreman A., Gottardi-Littell N., Van Broeckhoven C., Merchiers P., Spittaels K., Annaert W. and De Strooper B. (2003) Presenilins mutated at Asp-257 or Asp-385 restore Pen-2 expression and Nicastrin glycosylation but remain catalytically inactive in the absence of wild type Presenilin. *J. Biol. Chem.* **278**, 43 430–43 436.

Onishi M., Kinoshita S., Morikawa Y., Shibuya A., Phillips J., Lanier L. L., Gorman D. M., Nolan G. P., Miyajima A. and Kitamura T. (1996) Applications of retrovirus-mediated expression cloning. *Exp. Hematol.* **24**, 324–329.

Prokop S., Shirotani S., Edbauer D., Haass C. and Steiner H. (2004) Requirement of PEN-2 for stabilization of the presenilin NTF/CTF heterodimer within the gamma-secretase complex. *J. Biol. Chem.* **279**, 23 255–23 261.

Ratovitski T., Slunt H. H., Thinakaran G., Price D. L., Sisodia S. S. and Borchelt D. R. (1997) Endoproteolytic processing and stabilization of wild-type and mutant presenilin. *J. Biol. Chem.* **272**, 24 536–24 541.

Sai X., Kawamura Y. H,, Kokame K..*et al* (2002) Endoplasmic reticulum stress-inducible protein, Herp, enhances presenilin-mediated generation of amyloid {beta} protein . *J. Biol. Chem.* **277**, 12 915–12 920.

Sastre M., Steiner H., Fuchs K., Capell A., Multhaup G., Condron M. M., Teplow D. B. and Haass C. (2001) Presenilin-dependent γ-secretase processing of beta-amyloid precursor protein at a site corresponding to the S3 cleavage of Notch. *EMBO Rep.* **2**, 835–841.

Schroeter E. H., Ilagan M. X., Brunkan A. L. *et al.* (2003) A presenilin dimer at the core of the γ-secretase enzyme: insights from parallel analysis of Notch 1 and APP proteolysis. *Proc. Natl Acad. Sci. USA* **100**, 13 075–13 080.

Seiffert D., Bradley J. D., Rominger C. M. *et al.* (2000) Presenilin-1 and -2 are molecular targets for γ-secretase inhibitors. *J. Biol. Chem.* **275**, 34 086–34 091.

Selkoe D. J. (1999) Translating cell biology into therapeutic advances in Alzheimer's disease. *Nature* **399**, A23–A31.

Shearman M. S., Beher D., Clarke E. E., Lewis H. D., Harrison T., Hunt P., Nadin A., Smith A. L., Stevenson G. and Castro J. L. (2000) L-685,458, an aspartyl protease transition state mimic, is a potent inhibitor of amyloid β-protein precursor gamma-secretase activity. *Biochemistry* **39**, 8698–8704.

Steiner H., Kostka M., Romig H. *et al.* (2000) Glycine 384 is required for presenilin-1 function and is conserved in bacterial polytopic aspartyl proteases. *Nat. Cell Biol.* **2**, 848–851.

Steiner H., Winkler E., Edbauer D., Prokop S., Basset G., Yamasaki A., Kostka M. and Haass C. (2002) PEN-2 is an integral component of the γ-secretase complex required for coordinated expression of presenilin and nicastrin. *J. Biol. Chem.* **277**, 39 062–39 065.

Sudoh S., Kawamura Y., Sato S., Wang R., Saido T. C., Oyama F., Sakaki Y., Komano H. and Yanagisawa K. (1998) Presenilin 1 mutations linked to familial Alzheimer's disease increase the intracellular levels of amyloid β-protein 1–42 and its N-terminally truncated variant(s) which are generated at distinct sites. *J. Neurochem.* **71**, 1535–1543.

Takasugi N., Tomita T., Hayashi I., Tsuruoka M., Niimura M., Takahashi Y., Thinakaran G. and Iwatsubo T. (2003) The role of presenilin cofactors in the γ-secretase complex. *Nature* **422**, 438–441.

Thinakaran G., Borchelt D. R., Lee M. K. *et al.* (1996) Endoproteolysis of presenilin 1 and accumulation of processed derivatives in vivo. *Neuron* **17**, 181–190.

Thinakaran G., Harris C. L., Ratovitski T., Davenport F., Slunt H. H., Price D. L., Borchelt D. R. and Sisodia S. S. (1997) Evidence that levels of presenilins (PS1 and PS2) are coordinately regulated by competition for limiting cellular factors. *J. Biol. Chem.* **272**, 28 415–28 422.

Vassar R., Bennett B. D., Babu-Khan S. *et al.* (1999) β-secretase cleavage of Alzheimer's amyloid precursor protein by the transmembrane aspartic protease BACE. *Science* **286**, 735–741.

Weidemann A., Eggert S., Reinhard F. B., Vogel M., Paliga K., Baier G., Masters C. L., Beyreuther K. and Evin G. (2002) A novel epsilon-cleavage within the transmembrane domain of the Alzheimer amyloid precursor protein demonstrates homology with Notch processing. *Biochemistry* **41**, 2825–2835.

Weihofen A., Binns K., Lemberg M. K., Ashman K. and Martoglio B. (2002) Identification of signal peptide peptidase, a presenilin-type aspartic protease. *Science* **296**, 2215–2218.

Wolfe M. S., Xia W., Ostaszewski B. L., Diehl T. S., Kimberly W. T. and Selkoe D. J. (1999) Two transmembrane aspartates in presenilin-1 required for presenilin endoproteolysis and γ-secretase activity. *Nature* **398**, 513–517.

Yang D. S., Tandon A., Chen F. *et al.* (2002) Mature glycosylation and trafficking of nicastrin modulate its binding to presenilins. *J. Biol. Chem.* **277**, 28 135–28 142.

Yu G., Chen F., Nishimura M. *et al.* (2000a) Mutation of conserved aspartates affects maturation of both aspartate mutant and endogenous presenilin 1 and presenilin 2 complexes. *J. Biol. Chem.* **275**, 27 348–27 353.

Yu G., Nishimura M., Arawaka S. *et al.* (2000b) Nicastrin modulates presenilin-mediated notch/glp-1 signal transduction and βAPP processing. *Nature* **407**, 48–54.

Zhang Z., Nadeau P., Song W., Donoviel D., Yuan M., Bernstein A. and Yankner B. A. (2000) Presenilins are required for γ-secretase cleavage of β-APP and transmembrane cleavage of Notch-1. *Nat. Cell Biol.* **2**, 463–465.

The tissue plasminogen activator–plasmin system participates in the rewarding effect of morphine by regulating dopamine release

Taku Nagai*†, Kiyofumi Yamada*†‡§, Masako Yoshimura*, Kazuhiro Ishikawa*, Yoshiaki Miyamoto*, Kazuki Hashimoto‡, Yukihiro Noda*, Atsumi Nitta*, and Toshitaka Nabeshima*§

*Department of Neuropsychopharmacology and Hospital Pharmacy, Nagoya University Graduate School of Medicine, Nagoya 466-8560, Japan; and ‡Laboratory of Neuropsychopharmacology, Department of Clinical Pharmacy, Faculty of Pharmaceutical Sciences, Kanazawa University, Kanazawa 920-0934, Japan

Edited by Solomon H. Snyder, John Hopkins University School of Medicine, Baltimore, MD, and approved January 8, 2004 (received for review October 11, 2003)

Tissue plasminogen activator (tPA) is a serine protease that catalyzes the conversion of plasminogen (plg) to plasmin, which in turn functions to degrade extracellular matrix proteins in the central nervous system. The tPA-plasmin system plays a role in synaptic plasticity and remodeling. Here we show that this protease system participates in the rewarding effects of morphine by acutely regulating morphine-induced dopamine release in the nucleus accumbens (NAcc). A single morphine treatment induced tPA mRNA and protein expression in a naloxone-sensitive manner, which was associated with an increase in the enzyme activity in the NAcc. The acute effect of morphine in inducing tPA expression was diminished after repeated administration. Morphine-induced conditioned place preference and hyperlocomotion were significantly reduced in $tPA^{-/-}$ and $plg^{-/-}$ mice, being accompanied by a loss of morphine-induced dopamine release in the NAcc. The defect of morphine-induced dopamine release and hyperlocomotion in $tPA^{-/-}$ mice was reversed by microinjections of either exogenous tPA or plasmin into the NAcc. Our findings demonstrate a previously undescribed function of the tPA-plasmin system in regulating dopamine release, which is involved in the rewarding effects of morphine.

Extracellular proteases are expressed by neurons in the central nervous system (1–4), and their function can vary from potentiating neurotransmitter receptor function (5) to structural alterations associated with long-lasting forms of synaptic plasticity (6, 7). Tissue plasminogen activator (tPA) is a serine protease that catalyzes the conversion of plasminogen (plg) to plasmin and plays a role in fibrinolysis. In addition, tPA is abundantly expressed in the central nervous system (8–10), where this protease is stored in synaptic vesicles (11, 12), released into the extracellular space by a depolarization stimulus (11, 12), and then the expression of its mRNA is up-regulated (8, 12). Recent studies have demonstrated that tPA regulates a cascade of extracellular proteolytic activities involved in neurite outgrowth (13), cell migration (14, 15), long-term potentiation and depression (6, 16–18), learning and memory (9, 17, 18), excitotoxic cell death (19, 20), and regeneration or recovery from injury in the nervous system (21). These findings suggest that tPA is involved in the regulation of numerous aspects of synaptic plasticity and remodeling.

It is well known that drugs of abuse, including morphine, acutely modulate the activity of mesolimbic dopaminergic neurons, projecting from the ventral tegmental area (VTA) of the midbrain to the nucleus accumbens (NAcc) (22–24). Morphine increases dopaminergic neurotransmission in the NAcc via the activation of dopamine cells in the VTA, an area that possesses a high density of μ-opioid receptors. This activation results mainly from the disinhibition of inhibitory GABAergic (GABA, γ-aminobutyric acid) interneurons in the VTA (25, 26). The rewarding effects of morphine that are associated with enhanced dopamine release in the NAcc are related to its abuse. It has been proposed that activity-dependent synaptic plasticity and remodeling of the mesolimbic dopaminergic system play a crucial role in the development of drug dependence (27).

In the present study, we examined the role of the tPA-plasmin system in the rewarding effects of and dependence on morphine in mice with a targeted deletion of the tPA ($tPA^{-/-}$ mice) (28) and plg ($plg^{-/-}$ mice) genes (29). Our findings suggest that the tPA-plasmin system participates in the rewarding effects of morphine by acutely regulating morphine-induced dopamine release in the NAcc.

Materials and Methods

Animals. Male Wistar rats (7 weeks old) were obtained from Charles River Breeding Laboratories (Yokohama, Japan). Wild-type (C57BL/6J), $tPA^{-/-}$, and $plg^{-/-}$ mice were from The Jackson Laboratory. All animal care and use were in accordance with the National Institutes of Health Guide for the Care and Use of Laboratory Animals and were approved by the Institutional Animal Care and Use Committee of Nagoya University.

Real-Time RT-PCR. For the single morphine treatment, animals were given morphine hydrochloride (Shionogi Pharmaceutical, Osaka) at a dose of 10 mg/kg s.c., whereas for repeated treatment, they were subjected to a 5-day regimen in which increasing doses of morphine (10, 20, 30, 40, and 50 mg/kg s.c.) were injected twice a day and then challenged with morphine (10 mg/kg s.c.) on day 6. The levels of tPA mRNA were determined by real-time RT-PCR by using an ABI PRISM 7700 sequencer detector (PE Applied Biosystems). The primers used were as follows: 5′-AAGGAGGCTCACGTCAGACTGTA-3′ (forward), 5′-CCTGCACACAGCATGTTGCT-3′ (reverse), TaqMan probe, 5′-CAGCCGCTGTACCTCACAGCATCTGTTTAA-3′.

Immunoprecipitation and Immunoblot. Brain tissues were homogenized, and the supernatants were incubated with polyclonal goat anti-tPA antibodies (Santa Cruz Biotechnology), followed by protein G-Sepharose. The resulting immune complexes were resuspended in Laemli sample buffer. Immunoblots were probed with polyclonal rabbit anti-tPA antibodies (American Diagnostica, Greenwich, CT), followed by horseradish peroxidase-linked

This paper was submitted directly (Track II) to the PNAS office.

Abbreviations: plg, plasminogen; tPA, tissue plg activator; NAcc, nucleus accumbens; VTA, ventral tegmental area.

†T.N. and K.Y. contributed equally to this work.

§To whom correspondence may be addressed. E-mail: kyamada@p.kanazawa-u.ac.jp or tnabeshi@med.nagoya-u.ac.jp.

www.pnas.org/cgi/doi/10.1073/pnas.0306587101

anti-rabbit secondary antibodies. The enhanced chemiluminescence method (Amersham Pharmacia Biosciences) was used.

Zymography. Gel zymography was adapted from a procedure described previously (30). Ten percent polyacrylamide SDS gels were copolymerized with casein (1 mg/ml; Sigma) and plasminogen (15 μg/ml; Chromogenix, Molndal, Sweden). Brain tissues were homogenized in lysis buffer (50 mM Tris·HCl, pH 6.8/0.05% Triton X-100/2 mM EDTA) and assayed for protein content. Serial concentrations of the homogenate were loaded onto the gels and electrophoresed. After electrophoresis, the SDS was extracted from the gel by using 2.5% Triton X-100, and the gel was incubated for 1 h in 0.1 M Tris·HCl, pH 8.1, at 37°C, followed by staining with 0.125% Coomassie brilliant blue in 50% methanol/10% acetic acid. Destaining with the same solvent revealed a transparent zone of lysis against the dark protein background at 65 kDa corresponding to tPA. The enzymatic activity of tPA was analyzed with the ATTO Densitograph Software Library Lane Analyzer (Atto Instruments, Tokyo).

***In Situ* Hybridization.** Frozen sections (10 μm) were thawed on coverslips and used for *in situ* hybridization (31). pAtlas1A plasmid with rat tPA cDNA (BD Biosciences, Palo Alto, CA) was linearized with *Sac*I or *Kpn*I and used as a template for production of digoxigenin-labeled antisense cRNA (335 base) or sense cRNA (328 base) with T3 or T7 RNA polymerase (Promega).

Immunohistochemistry. Sections (14 μm) were incubated with polyclonal rabbit anti-tPA (1:1,000, Molecular Innovations, Southfield, MI) and monoclonal mouse antimicrotubule-associated protein 2 (MAP2) antibodies (1:5,000, Sigma), in blocking serum containing goat anti-rabbit Alexa Fluor 546 (1:500, Molecular Probes) and goat anti-mouse Alexa Fluor 488 (1:1,000, Molecular Probes). Samples were observed with AXIOVISION 3.0 systems (Zeiss).

***In Vivo* Microdialysis.** Animals were anesthetized with sodium pentobarbital, and a guide cannula (AG-8, EICOM, Kyoto) was implanted in the NAcc (AP +1.1, ML +1.0 from bregma, DV −3.6 from the skull) according to the atlas (32). Two days after the operation, a dialysis probe (AI-8–1; 1-mm membrane length, EICOM) was inserted through a guide cannula and perfused with an artificial cerebrospinal fluid (aCSF; 147 mM NaCl/4 mM KCl/2.3 mM $CaCl_2$) at a flow rate of 1.0 μl/min. The outflow fractions were collected every 20 min. After the collection of three baseline fractions, mice were treated with morphine (10 mg/kg s.c.). For depolarization stimulation, 60 mM KCl containing aCSF was delivered through the dialysis probe for 20 min. Dopamine levels in the dialysates were analyzed as described (33). For the rescue study with tPA and plasmin, a dialysis probe equipped with a microinjection tube (MIA-8–1; 1 mm membrane length, EICOM) was used (34). After the collection of baseline fractions, a 100-ng dose of human recombinant tPA (provided by Eisai, Tokyo) or 0.01 unit dose of human plasmin (Chromogenix) dissolved in 1 μl of aCSF solution was injected during a 10-min period through the microinjection tube into the NAcc. Ten minutes after the microinjection, mice were treated with morphine.

Behavioral Analysis. For the acute locomotor-stimulating effect, $tPA^{-/-}$ and wild-type mice were injected with saline or morphine (10 mg/kg s.c.) on day 1, and the locomotor activity was measured for 180 min. For the sensitization, mice were injected with morphine (10 mg/kg s.c.) twice per day for 5 days from days 2 to 6, and morphine-induced locomotor activity was measured on day 16. For the rescue study with tPA and plasmin, a guide cannula was implanted in the NAcc (AP +1.1, ML ±1.0 from bregma, DV −3.6 from the skull). After recovery from the operation, tPA (100 ng) or human plasmin (0.01 units) was injected through the microinjection tube into the NAcc. Ten minutes after the microinjection, mice were treated with morphine (10 mg/kg s.c.), and the locomotor activity was measured for 180 min.

For the conditioned place preference test (35), a mouse was allowed to move freely between transparent and black boxes for 15 min once per day for 3 days (days 1–3) in the preconditioning. On day 3, the time the mouse spent in each box was measured. On days 4, 6, and 8, the mouse was treated with morphine and confined in either the transparent or black box for 30 min. On days 5, 7, and 9, the mouse was given saline and placed opposite to the morphine-conditioning box for 30 min. On day 10, the postconditioning test was performed without drug treatment, and the time the mouse spent in each box was measured for 15 min.

For the hot-plate test (36), nociceptive latency was assessed as the response time to the hot plate (55 ± 1°C). To avoid tissue damage, an artificial maximum time for exposure was imposed, which prevented the animal from making contact with the plate for >30 sec.

Statistical Analysis. Statistical analysis was performed by using ANOVA and the Bonferroni test. The Mann–Whitney *U* test was used to compare two sets of data. Data were expressed as the mean ± SE. *P* values of <0.05 were considered statistically significant.

Results

Morphine-Induced tPA mRNA Expression in the Brain. The effects of single and repeated administration of morphine on the expression of tPA mRNA in various regions of the rat brain were measured 2 h after the final morphine treatment by a real-time RT-PCR method. Single morphine treatment remarkably induced the tPA mRNA expression compared with saline treatment in the frontal cortex (FC, 257% of control, $P < 0.01$), NAcc (772%, $P < 0.01$), striatum (STR, 535%, $P < 0.01$), hippocampus (HIP, 799%, $P < 0.01$), VTA (337%, $P < 0.01$), and amygdala (AMY, 332%, $P < 0.01$) (Fig. 1*A*). Although the effect of morphine on tPA mRNA expression was significantly reduced after repeated treatment, expression levels were significantly higher in the repeated morphine-treated group than control group in the FC (146%, $P < 0.05$), NAcc (150%, $P < 0.05$), STR (143%, $P < 0.05$), and HIP (248%, $P < 0.01$) (Fig. 1*A*). Because it is known that there are some species differences in the effect of morphine, we also examined the effect of morphine on tPA expression in mice. The levels of tPA mRNA were significantly increased in the NAcc of mice 1 h (158% of control, $P < 0.01$), 2 h (179%, $P < 0.01$), and 6 h (140%, $P < 0.05$) after morphine treatment and then returned to the control value 24 h later [$F_{(6, 35)} = 4.401$, $P < 0.01$, Fig. 1*B*]. The protein levels of tPA determined by Western blotting were also significantly increased 6 h (147%, $P < 0.05$), 24 h (155%, $P < 0.01$), and 48 h (143%, $P < 0.05$) after single morphine treatment and then returned to the control value 1 week after the treatment [$F_{(6, 42)} = 3.384$, $P < 0.01$, Fig. 1*C*]. The enzymatic activity of tPA, which was assayed by gel zymography (30), was significantly increased compared with the saline-treated group 1 h (145%, $P < 0.01$), 2 h (139%, $P < 0.01$), 6 h (126%, $P < 0.05$), and 48 h (128%, $P < 0.05$) after the morphine treatment [$F_{(6,28)} = 3.733$, $P < 0.01$, Fig. 1*D*]. No enzymatic activity of tPA was detected in $tPA^{-/-}$ mice (Fig. 1*D*). Morphine-induced tPA activity was completely inhibited by pretreatment with naloxone (1 mg/kg i.p.), although naloxone itself had no effect, suggesting the involvement of opioid receptors in the morphine-induced increase in tPA activity (Fig. 1*E*).

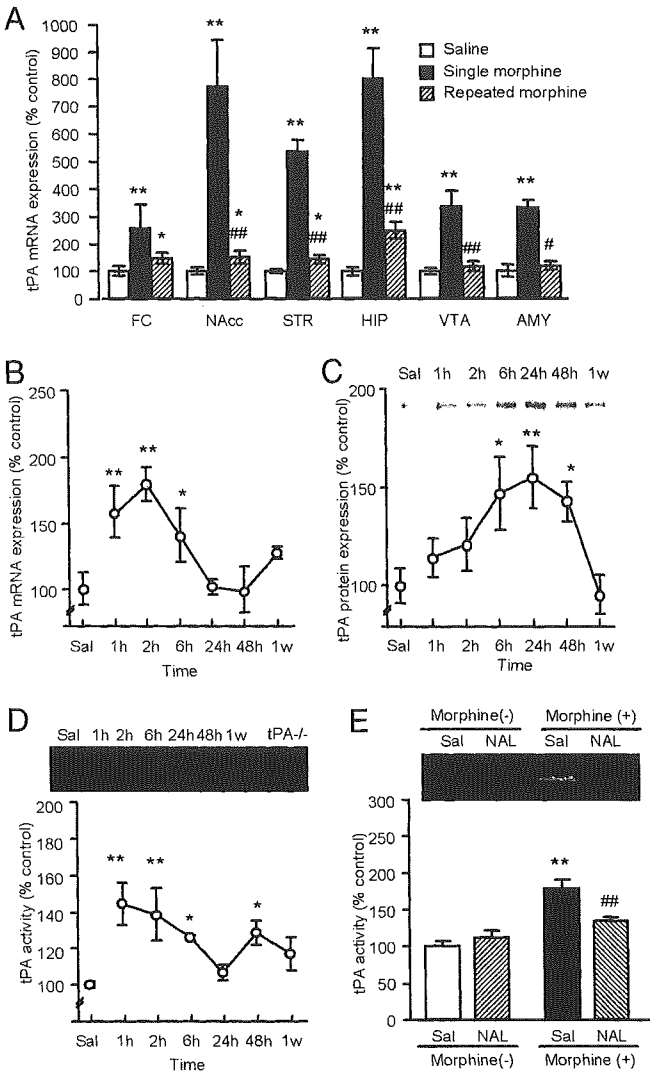

Fig. 1. Increased tPA expression after morphine treatment. (*A*) Changes in tPA mRNA expression after single (10 mg/kg s.c.) and repeated (10–50 mg/kg × 2 per day s.c.) morphine treatment in the rat brain. (*B*) Time course changes in tPA mRNA expression after single morphine (10 mg/kg s.c.) treatment in the NAcc of mice. (*C*) Immunoprecipitation/immunoblot analysis of tPA protein. (*D*) Zymographic analysis of tPA activity. (*E*) Effect of naloxone on single morphine-induced tPA activity. Values indicate means ± SE (n = 9–10 for *A*, n = 6 for *B*, n = 7 for *C*, n = 6 for *D*, and n = 4 for *E*). *, $P < 0.05$ and **, $P < 0.01$ compared with the saline (Sal)-treated group. #, $P < 0.05$ and ##, $P < 0.01$ compared with the single morphine-treated group.

Morphine-Induced tPA Is Produced in Neurons of the NAcc. It has been reported that tPA mRNA is present in both neurons and microglia but not oligodendrocytes or astrocytes (10, 19). To determine the cell types in which tPA expression is induced by acute morphine treatment, *in situ* hybridization with antisense tPA digoxigenin-labeled RNA probes as well as immunohistochemistry with specific tPA antibodies was performed (Fig. 2). The tPA mRNA was detected in cells of the NAcc in both saline- and morphine-treated wild-type mice (Fig. 2 *A* and *B*), but the signals in morphine-treated animals were apparently more intense than those in saline-treated animals. No signals were detected in the brain sections of $tPA^{-/-}$ mice (Fig. 2*C*). Immunohistochemistry revealed that tPA immunoreactivity was localized to cells positive for MAP2, a marker of neuronal cells (Fig. 2 *D–F*), indicating that tPA is produced in neuronal cells after morphine treatment.

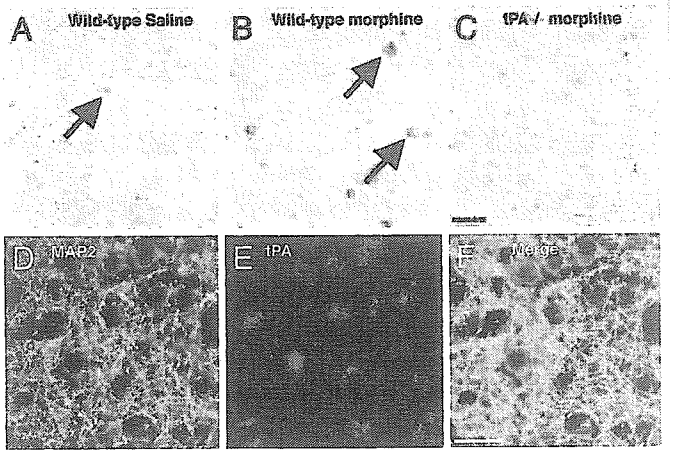

Fig. 2. tPA expression in the NAcc after morphine treatment. *In situ* hybridization analysis of tPA mRNA expression in the NAcc of saline-treated wild-type mice (*A*), morphine-treated wild-type mice (*B*), and morphine-treated $tPA^{-/-}$ mice (*C*). (*D–F*) Immunohistochemical analysis of morphine-induced tPA expression in the NAcc of mice. (*D*) MAP2. (*E*) tPA. (*F*) Merge. (Bar = 20 μm.)

No Changes in Antinociceptive Effects of Morphine and Tolerance in $tPA^{-/-}$ Mice. To investigate the physiological significance of the morphine-induced increase in tPA expression, we examined the antinociceptive effect of morphine and the development of its tolerance (36) in $tPA^{-/-}$ mice. There were no differences in the basal antinociceptive threshold between wild-type and $tPA^{-/-}$ mice in the hot-plate test (wild-type, 4.4 ± 0.5 sec; $tPA^{-/-}$, 4.6 ± 0.5 sec). No differences were observed either in the acute morphine-induced antinociceptive effect between wild-type and $tPA^{-/-}$ mice. Repeated injections of morphine (10 mg/kg × 2 per day s.c.) for 5 days resulted in a gradual loss of the antinociceptive effects of morphine in both wild-type and $tPA^{-/-}$ mice, and there were no differences at all in the time course (Fig. 3*A*). These results suggest that tPA has little effect on morphine-induced antinociception and its tolerance after repeated administration.

Morphine-Induced Behavioral Effects in $tPA^{-/-}$ and $plg^{-/-}$ Mice. Because we observed marked changes in tPA expression and activity in the NAcc, a brain area important for the rewarding effects of drugs of abuse (24, 27), we focused on the role of the tPA-plasmin system in the rewarding effects of morphine, which can be assessed by using the conditioned place-preference test (35). Morphine induced a dose-dependent conditioned place preference in wild-type mice, whereas saline treatment had no effect on place preference [$F_{(2, 48)} = 11.811$, $P < 0.01$, Fig. 3*B*]. Interestingly, the rewarding effects of morphine were markedly reduced in $tPA^{-/-}$ mice at the conditioning doses of 3 and 10 mg/kg ($P < 0.05$, Fig. 3*B*). Moreover, morphine (10 mg/kg s.c.) failed to induce place preference in $plg^{-/-}$ mice ($P < 0.05$, Fig. 3*C*), suggesting a role for the tPA-plasmin system in the rewarding effects of morphine.

The NAcc is involved not only in rewarding effects but also in locomotor-stimulating effects of morphine (22). Therefore, we measured the locomotor-stimulating effects of morphine in $tPA^{-/-}$ mice. Single morphine (10 mg/kg s.c.) treatment induced a hyperlocomotion in wild-type mice and $tPA^{-/-}$ mice, but the magnitude was significantly reduced in $tPA^{-/-}$ mice compared with wild-type mice ($P < 0.05$, Fig. 3*D*). Although repeated morphine treatment significantly potentiated the locomotor-stimulating effects of morphine in wild-type mice ($P < 0.01$), it failed to potentiate the hyperlocomotion in $tPA^{-/-}$ mice (Fig. 3*D*). We also examined whether exogenous tPA and plasmin can reverse the defect of loco-

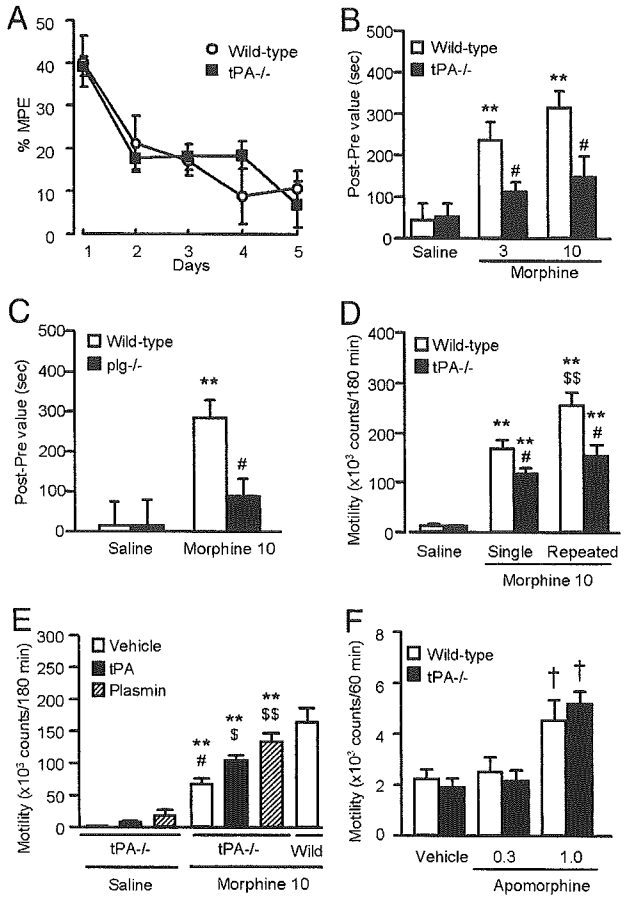

Fig. 3. Morphine-induced behavioral effects in $tPA^{-/-}$ and $plg^{-/-}$ mice. (*A*) Development of tolerance to the antinociceptive effect of morphine (10 mg/kg s.c.) in $tPA^{-/-}$ mice. (*B* and *C*) Morphine (3 and 10 mg/kg s.c.)-induced place preference in $tPA^{-/-}$ mice (*B*) and $plg^{-/-}$ mice (*C*). (*D*) Locomotor activity and locomotor sensitization induced by morphine (10 mg/kg s.c.) treatment. (*E*) Effect of tPA and plasmin microinjection into the NAcc on locomotor activity induced by morphine (10 mg/kg s.c.) in the $tPA^{-/-}$ mice. (*F*) Apomorphine (0.3 and 1.0 mg/kg s.c.)-induced hyperlocomotion. Values indicate means ± SE (n = 4–5 for *A*, n = 8–21 for *B*, n = 6–12 for *C*, n = 10 for *D*, n = 8 for *E*, and n = 8 for *F*). *, $P < 0.05$ and **, $P < 0.01$ compared to corresponding saline-treated mice. #, $P < 0.05$ compared to corresponding morphine-treated wild-type mice. $, $P < 0.05$ and $$, $P < 0.01$ compared to vehicle plus morphine-treated $tPA^{-/-}$ mice. †, $P < 0.05$ compared to corresponding vehicle-treated mice.

motor-stimulating effect of morphine in $tPA^{-/-}$ mice. The attenuation of hyperlocomotion in $tPA^{-/-}$ mice was significantly reversed by microinjections of either exogenous tPA (100 ng, $P < 0.05$) or plasmin (0.01 units, $P < 0.01$) into the NAcc [$F_{(6, 49)} = 32.824$, $P < 0.01$, Fig. 3*E*].

The reduction of these behavioral effects of morphine in $tPA^{-/-}$ and $plg^{-/-}$ mice might be due to the alteration of dopamine and/or opioid receptor sensitivity. To test this possibility, we studied locomotor responses to different doses of apomorphine, a direct dopamine D1/D2 receptor agonist. In wild-type mice, apomorphine (0.3 and 1.0 mg/kg s.c.) significantly increased locomotor activities in a dose-dependent manner [$F_{(2, 21)} = 4.389$, $P < 0.05$], and there were no differences in apomorphine-induced hyperlocomotion between wild-type and $tPA^{-/-}$ mice (Fig. 3*F*). We also measured dopamine- and morphine-induced stimulation of [^{35}S]GTPγS binding in membrane preparation *in vitro*. The dopamine- and morphine-induced [^{35}S]GTPγS binding in $tPA^{-/-}$ mice did not differ from those in wild-type mice (Fig. 6, which is published as supporting information on the PNAS web site). These results indicate that the tPA-plasmin system plays a crucial role in morphine-induced rewarding and locomotor stimulating effects, and that these behavioral changes in $tPA^{-/-}$ mice are not due to alterations of dopamine and opioid receptor sensitivity.

Role of tPA in Morphine-Induced Dopamine Release in the NAcc. It has been suggested that the enhancement of dopamine release in the NAcc is an essential process related to the morphine-induced rewarding effect (37). To clarify the mechanisms by which $tPA^{-/-}$ mice exhibited the reduced morphine-induced rewarding and locomotor-stimulating effects, we measured morphine-induced dopamine release in the NAcc. *In vivo* microdialysis revealed that basal levels of dopamine in the NAcc were not different between wild-type and $tPA^{-/-}$ mice (wild-type, 0.41 ± 0.13 nM, n = 4; $tPA^{-/-}$, 0.53 ± 0.01 nM, n = 4). The dopamine levels in the NAcc were markedly increased by s.c. injection of morphine at 10 mg/kg in wild-type mice (Fig. 4*A*). This morphine-induced dopamine release was markedly diminished in $tPA^{-/-}$ mice [$F_{(1, 6)} = 13.061$, $P < 0.05$, Fig. 4*A*]. Similarly, although basal levels of dopamine in the NAcc of $plg^{-/-}$ mice did not differ from those in wild-type mice (wild-type, 0.38 ± 0.10 nM, n = 6; $plg^{-/-}$, 0.38 ± 0.05 nM, n = 6), morphine-induced dopamine release in the NAcc was significantly reduced in $plg^{-/-}$ mice compared to wild-type mice [$F_{(1, 10)} = 25.147$, $P < 0.01$, Fig. 4*B*].

We investigated the mechanisms underlying the defect of morphine-induced dopamine release in $tPA^{-/-}$ mice and $plg^{-/-}$ mice. Microinjection of tPA (100 ng) into the NAcc slightly but significantly increased basal levels of extracellular dopamine in $tPA^{-/-}$ mice [$F_{(1, 8)} = 7.941$, $P < 0.05$, Fig. 4*C*]. Further, this pretreatment dramatically increased morphine-induced dopamine release in $tPA^{-/-}$ mice as observed in wild-type mice [$F_{(1, 8)} = 5.428$, $P < 0.05$, Fig. 4*D*]. In contrast, microinjection of tPA (100 ng) into the VTA failed to increase morphine-induced dopamine release in the NAcc of $tPA^{-/-}$ mice (Fig. 7, which is published as supporting information on the PNAS web site). These results suggest that the defect of morphine-induced dopamine release in $tPA^{-/-}$ mice is due to the deficiency of tPA in the NAcc, not to a developmental malfunction. Microinjection of plasmin (0.01 units) into the NAcc caused a transient but significant increase in basal dopamine levels in $tPA^{-/-}$ mice [$F_{(1, 8)} = 6.612$, $P < 0.05$, Fig. 4*E*]. Moreover, this pretreatment markedly increased morphine-induced dopamine release in $tPA^{-/-}$ mice [$F_{(1, 8)} = 13.121$, $P < 0.01$, Fig. 4*F*]. These results suggest that tPA modulates morphine-induced dopamine release probably by converting plg to plasmin in the NAcc.

Because tPA is released into the extracellular space by a depolarization stimulus (11, 12), we investigated the depolarization (60 mM KCl)-evoked dopamine release in the NAcc of $tPA^{-/-}$ mice. The lack of tPA significantly attenuated the depolarization-evoked dopamine release in the NAcc [$F_{(1, 10)} = 6.846$, $P < 0.05$, Fig. 5*A*]. There were no differences in the protein content of tyrosine hydroxylase in the NAcc and lower midbrain, a rate limiting enzyme of dopamine synthesis, between $tPA^{-/-}$ and wild-type mice (Fig. 5*B*).

Discussion

It has been demonstrated that tPA takes part in the proteolysis of extracellular matrix proteins in the central nervous system and is involved in neuronal plasticity. In the present study, we demonstrated a previously undescribed function of the tPA-plasmin system in regulating dopamine release in the NAcc. Furthermore, the tPA-plasmin system is involved in the rewarding effects of morphine by regulating dopamine release.